

# ELECTRICAL DISCHARGE TEXTURING OF CUTTING TOOLS

# ELECTRICAL DISCHARGE TEXTURING OF CUTTING TOOLS

By

JOSH M. TOVEY, B.ENG.

A Thesis

Submitted to the School of Graduate Studies

In Partial Fulfillment of the Requirements

For the Degree

Master of Applied Science

McMaster University

©Copyright by Josh M. Tovey, September 2010

MASTER OF APPLIED SCIENCE (2010)

McMaster University

(Department of Mechanical Engineering)

Hamilton, Ontario

TITLE: Electrical Discharge Texturing of Cutting Tools

AUTHOR: Josh Tovey, B.Eng. (McMaster University)

SUPERVISOR: Dr. Philip Koshy

NUMBER OF PAGES: xiii, 104

## **Abstract**

During metal removal operations, friction occurs at the interface between the rake face of the cutting tool and the chip. Tool rake face friction adversely influences the chip formation process and consumes about 25% of the total cutting energy. Friction in cutting can be controlled and reduced by introducing a lubricant into the tool-chip interface, however the effectiveness of this is a function of the cutting speed and uncut chip thickness, among other factors. Lubricant penetration was determined in the 1970's to be a result of capillary action through channels resulting in part from the roughness of the tool rake face and the mating chip face. Recent investigations have looked at increasing the penetration and effectiveness of lubrication by engineering the tool surface to promote and retain lubricants by introducing a texture on the tool rake face.

This thesis details methods used for surface engineering the rake face of cutting tools focusing on the novel application of electrical discharge machining (EDM) to obtain the desired texture, with a view to facilitating lubricant penetration and retention. A significant enhancement in machining performance consequent to such tool face texturing is demonstrated. The functionality of such surfaces is discussed as well as the texturing process, application areas and limitations.

## Acknowledgements

There have been many people that have contributed in making this work possible and I would like to take a moment to recognize their contributions and assistance.

First I would like to thank Dr. Koshy for his guidance and positive attitude towards this thesis and teaching in general. He has been a very positive influence since first taking his second year undergraduate mechanics course, and has provided much support and encouragement, both as a supervisor and a friend, as well as many competitive squash games, only a few of which I have won.

Second I would like to thank the support of all my friends and family, who were able to help me recharge and forget about school when needed. To my parents Martin and Heather, and my sister Katelyn, in 3 years I will be reading your thesis. I have some amazing friends from home that have encouraged me, and have made a few new ones while completing this degree who have made my stay in Hamilton and at McMaster University quite enjoyable.

Thanks to the other members of my research group and associates, Nick Trutwin, Andrew Biksa, Youseff Ziada, Ryan Babel, and Nima Zarif for allowing the fruitful discussion of ideas, as well as many laughs throughout the work day.

I would also like to acknowledge the behind the scenes faculty at McMaster University without them this thesis could not be completed. Special thanks to J.P. Talon whose technical support as well as positive attitude in the machine shop allowed for the

preparation of parts and samples needed in this thesis, and humorous demeanor provided countless entertaining and insightful discussions throughout the day.

*Dedicated to all my family and friends who have helped make this possible*

# Table of Contents

<b>Abstract</b> .....	<b>iii</b>
<b>Acknowledgements</b> .....	<b>iv</b>
<b>List of Figures</b> .....	<b>x</b>
<b>List of Tables</b> .....	<b>xiv</b>
<b>Chapter 1 Introduction</b> .....	<b>1</b>
1.1 Metal Cutting Basics .....	2
1.2 Friction in Cutting .....	8
1.3 Friction Reduction .....	9
1.3.1 Coatings.....	10
1.3.2 Cutting Fluids .....	10
1.4 Scope and Organization of Project.....	12
<b>Chapter 2 Literature Review</b> .....	<b>13</b>
2.1 Lubrication in Metal Cutting.....	13
2.1.1 How Lubricants Work .....	14
2.1.2 Application of Lubricants.....	19
2.1.3 Effect of Cutting Parameters .....	21
2.1.4 Dependence on Asperity Contact for Lubrication.....	24
2.2 Engineered Surfaces .....	25
2.2.1 Dimpled Textures .....	25
2.2.2 Linear Textures.....	32
2.3 Texturing Processes.....	35
2.3.1 Laser Surface Texturing .....	36
2.3.2 Electrochemical Machining.....	38
2.3.3 Other Processes .....	39
2.4 EDM Texturing .....	40
2.4.1 Previous Work with EDM.....	40

2.4.2 How EDM Works.....	41
<b>Chapter 3 Experimental Details.....</b>	<b>45</b>
3.1 EDM Setup.....	45
3.2 Textured Cutting Inserts.....	46
3.2.1 Cutting Inserts.....	46
3.2.2 Dimpled Texturing of Cutting Inserts.....	47
3.2.3 Linear Textured Inserts.....	48
3.2.4 Texture Characterization.....	49
3.3 Experimental Test Setup.....	49
3.3.1 Oil Supply.....	51
3.3.2 Calibration.....	52
3.3.3 Test Samples.....	53
3.3.4 Interrupted Cutting.....	54
3.4 Test Procedure.....	55
3.4.1 Preliminary Testing.....	55
3.4.2 Non-Textured Edge Testing.....	56
3.4.3 Tool Chip Contact Length.....	58
3.4.4 EDM Parameter Comparison.....	58
3.4.5 Linear Textures.....	59
3.4.6 Cutting Parameters.....	60
3.5 Surface Roughness.....	60
<b>Chapter 4 Results and Discussion.....</b>	<b>61</b>
4.1 Force Relation Between Measured Forces and Tool Forces.....	62
4.2 Force Time Plots for Lubricated and Non Lubricated Cutting.....	63
4.3 Effect of Textures on Continuous and Interrupted Cutting.....	66
4.3.1 Continuous Cutting.....	66
4.3.2 Interrupted Cutting.....	67

4.4 Components of Force Reduction when using Textured Inserts.....	70
4.5 Texture Geometry.....	73
4.5.1 Texture Location .....	73
4.5.2 Contact Length Test .....	76
4.5.3 Linear Textures.....	79
4.5.4 Effect of EDM Parameters .....	82
4.6 Cutting Parameters .....	87
4.6.1 Effect of Cutting Speed and Feed in Continuous Cutting .....	87
4.6.2 Effect of Cutting Speed – Continuous and Interrupted Cutting Comparison	89
4.6.3 Engagement Length.....	90
4.6.4 Testing on Aluminum Workpiece .....	92
4.6.5 Texture Location When Cutting Aluminum.....	93
4.7 Workpiece Surface Roughness.....	94
<b>Chapter 5 Conclusions and Future Work .....</b>	<b>96</b>
5.1 Conclusion.....	96
5.2 Future Work.....	98
<b>References .....</b>	<b>100</b>

## List of Figures

Figure 1.1 Basic Metal Cutting Operations Showing Chip Formation [1] .....	2
Figure 1.2. Geometry of Orthogonal Cutting.....	3
Figure 1.3. Deformation Zones in Cutting.....	4
Figure 1.4. Free Body Diagram of Chip .....	6
Figure 1.5. Merchant's Circle Diagram.....	7
Figure 1.6. Localized Contact of Asperities .....	8
Figure 2.1. Real and Apparent Contact.....	14
Figure 2.2. Sliding Between Surfaces with Solid Lubricant Layer .....	15
Figure 2.3. Split Tool to Measure Cutting Forces .....	17
Figure 2.4. Stress Distribution on Rake Face of Cutting Tool.....	18
Figure 2.5. Fluid Penetration Through Micro Channels of Length L at Interface [9] .....	19
Figure 2.6. Effect of Carbon Tetrachloride as a Lubricant in a Copper Turning Experiment [9] .....	22
Figure 2.7 Lubrication Range as a Function of Uncut Chip Thickness and Cutting Speed [9].....	23
Figure 2.8 Representative Dimpled Texture [28]. .....	26
Figure 2.9. Characteristic Stribeck Diagram.....	30
Figure 2.10. Linear Textures on Cutting Tools [32].....	33
Figure 2.11. Cutting Forces Based on Scale of Texturing [32]. .....	33
Figure 2.12. Performance of Textured Tool [32].....	34
Figure 2.13 Example Laser Textured Surface [28].....	36
Figure 2.14. Laser Surface Dimpling and Corresponding Formtracer Profile [23].....	37
Figure 2.15 Through-Mask Electrochemical Machining [25]. .....	38
Figure 2.16. Dimpled Pattern as a Result of ECM [25].....	39
Figure 2.17 EDM Micro Hole on Rake Face of Cutting Tool [36]. .....	41
Figure 2.18. EDM Process .....	42

Figure 2.19. Positive and Negatively Skewed Surfaces .....	42
Figure 3.1. Aigetron Impact 2 Ram EDM .....	46
Figure 3.2. Insert Texturing Setup .....	47
Figure 3.3. Insert Showing Textured Region.....	48
Figure 3.4. Linear Textured Insert with Textured and Non Textured Cutting Edge .....	49
Figure 3.5. Nakamura Tome Sc-459 Lathe Test Setup.....	50
Figure 3.6. Oil Supply Direction.....	51
Figure 3.7. Dimensions of Workpiece .....	53
Figure 3.8. Ribbed 1045 Steel Test Sample.....	54
Figure 3.9. Cross Section of Interrupted Test Samples Showing the Slots .....	55
Figure 3.10. Interrupted Cutting Test Sample.....	55
Figure 3.11. Definition of Non Textured Gap Size X.....	57
Figure 3.12. Progression of Non Textured Gap Size .....	57
Figure 4.1. Flow Chart Outlining Experimental Work Presented in Chapter 4.....	61
Figure 4.2. Merchant's Circle Diagram.....	62
Figure 4.3. Merchants Circle Diagram with $\alpha = 0^\circ$ .....	63
Figure 4.4. Comparison of Feed Force between Non Textured and Textured Inserts – Continuous Cutting 1045 Steel $t = 0.1$ mm $V_c = 2$ m/min $X = 0.2$ mm.....	64
Figure 4.5. Comparison of Cutting Force between Non Textured and Textured Inserts – Continuous Cutting 1045 Steel $t = 0.1$ mm $V_c = 2$ m/min $X = 0.2$ mm.....	65
Figure 4.6. Average Feed and Cutting Force Comparison of Inserts - Continuous Cutting 1045 Steel $t = 0.1$ mm $V_c = 2$ m/min $X = 0.2$ mm .....	67
Figure 4.7. Feed Force Comparison between Textured and Non Textured Inserts – Interrupted Cutting 1045 Steel $t = 0.1$ mm $V_c = 2$ m/min $X = 0.2$ mm .....	69
Figure 4.8. Cutting Force Comparison between Textured and Non Textured Inserts – Interrupted Cutting 1045 Steel $t = 0.1$ mm $V_c = 2$ m/min $X = 0.2$ mm .....	69
Figure 4.9. Feed and Cutting Force Comparison of Inserts - Interrupted Cutting 1045 Steel $t = 0.1$ mm $V_c = 2$ m/min $X = 0.2$ mm .....	70
Figure 4.10 Percent Reduction in Feed and Cutting Force Due to Forms of Cutting – Continuous and Interrupted Cutting 1045 Steel $t = 0.1$ mm $V_c = 2$ m/min $X = 0.2$ mm ..	71

Figure 4.11. Percent Reduction in Feed and Cutting Force Due to Aspects of the Texture - Continuous and Interrupted Cutting 1045 Steel $t = 0.1$ mm $V_c = 2$ m/min $X = 0.2$ mm ..	72
Figure 4.12 Texture Location with Respect to Cutting Edge .....	74
Figure 4.13. Percent Reduction of Feed Force as a Result of Uncut Chip Thickness and Non Textured Edge Length $X$ - Continuous Cutting 1045 Steel $V_c = 2$ m/min.....	74
Figure 4.14 Friction Angle as a Result of Uncut Chip Thickness and $X$ - Continuous Cutting 1045 Steel $V_c = 2$ m/min .....	75
Figure 4.15 Result of Impingement of Chip on Rake Face of Textured Insert - Continuous Cutting 1045 Steel $t = 1$ mm $V_c = 2$ m/min $X = 0.2$ mm .....	77
Figure 4.16 Increased Percent of Surface Textured.....	79
Figure 4.17. Reduction in Feed Force as a Function of Surface Area Textured - Continuous Cutting 1045 Steel $t = 0.1$ mm $V_c = 2$ m/min $X = 0.2$ mm.....	80
Figure 4.18. Reduction in Cutting Force as a Function of Surface Area Textured- Continuous Cutting 1045 Steel $t = 0.1$ mm $V_c = 2$ m/min $X = 0.2$ mm.....	80
Figure 4.19 Comparison Between Linear Texture and Solid Texture .....	81
Figure 4.20. Insert Damaged During Cutting .....	82
Figure 4.21. Percent Reduction in Force as a Result of Current – Pulse on Time at $42 \mu$ s Continuous Cutting 1045 Steel $t = 0.1$ mm $V_c = 2$ m/min $X = 0.2$ mm.....	83
Figure 4.22. Percent Reduction in Force as a Result of Pulse On – Time – Current at 39 amps Continuous Cutting 1045 Steel $t = 0.1$ mm $V_c = 2$ m/min $X = 0.2$ mm .....	83
Figure 4.23. Percent Reduction of Feed Force as a Result of Texture Roughness $R_a$ - Continuous Cutting 1045 Steel $t = 0.1$ mm $V_c = 2$ m/min $X = 0.2$ mm.....	85
Figure 4.24. Percent Reduction of Feed Force as a Result of Texture Skewness - Continuous Cutting 1045 Steel $t = 0.1$ mm $V_c = 2$ m/min $X = 0.2$ mm.....	86
Figure 4.25. Percent Reduction of Cutting Force as a Result of Kurtosis - Continuous Cutting 1045 Steel $t = 0.1$ mm $V_c = 2$ m/min $X = 0.2$ mm .....	86
Figure 4.26. Percent Reduction in Feed Force as a Function of Uncut Chip Thickness and Cutting Speed– Continuous Cutting 1045 Steel $X = 0.06$ mm.....	88
Figure 4.27. Percent Reduction in Cutting Force as a Function of Uncut Chip Thickness with an Increase in Cutting Speed– Continuous Cutting 1045 Steel $X = 0.06$ mm.....	88
Figure 4.28 Percent Reduction in Feed and Cutting Force as a Function of Cutting Speed - Continuous and Interrupted Cutting 1045 Steel $t = 0.1$ mm $X = 0.2$ mm .....	90

Figure 4.29. Percent Reduction in Average Feed and Cutting Force based on Length of Test – Interrupted Cutting 1045 Steel $t = 0.1$ mm $V_c = 2$ m/min $X = 0.40$ mm.....	91
Figure 4.30. Feed Force Comparison between Textured and Non Textured Inserts – Continuous Cutting 6061 Aluminum $t = 0.15$ mm $V_c = 2$ m/min $X = 0.2$ mm .....	92
Figure 4.31 Cutting Force Comparison between Textured and Non Textured Inserts – Continuous Cutting 6061 Aluminum $t = 0.15$ mm $V_c = 2$ m/min $X = 0.2$ mm .....	93
Figure 4.32 Percent Reduction in Feed and Cutting Force as a Function of Uncut Chip Thickness– Continuous Cutting 6061 Aluminum $V_c = 2$ m/min $X = 0.2$ mm.....	94
Figure 4.33 Surface Roughness $R_a(\mu\text{m})$ at Different Uncut Chip Thickness– Continuous Cutting 1045 Steel $V_c = 2$ m/min .....	95

## List of Tables

Table 3.1. Properties of Chem Ecol 250 A Cutting Oil .....	50
Table 3.2. Cutting Forces with Various Nozzle Configurations Continuous Cutting 1045 Steel $t = 0.1$ mm $V_c = 2$ m/min $X = 0.2$ mm.....	52
Table 3.3. Cutting Parameters of Initially Tested Insert.....	56
Table 3.4. EDM Parameter Testing .....	59
Table 3.5. Linear Texture Configuration .....	59
Table 4.1. Engagement Length of Interrupted Test .....	68
Table 4.2. Chip Contact Length Comparison at Uncut Chip Thickness of 0.025 mm - Continuous Cutting 1045 Steel $V_c = 2$ m/min $X = 0.09$ mm .....	78
Table 4.3. Chip Contact Length Comparison at Uncut Chip Thickness of 0.1 mm - Continuous Cutting 1045 Steel $V_c = 2$ m/min $X = 0.2$ mm .....	78
Table 4.4 Surface Characteristics as a Function of EDM Parameters .....	84
Table 4.5. Engagement Length of Test.....	91

## Chapter 1

### Introduction

The industrial trend in machining over the last couple decades has been a move towards miniaturization and sustainability. Dwindling resources coupled with increasing energy prices have promoted industrial processes that are more efficient. In machining processes this trend has been towards machines that are more efficient and smaller while still having the same capabilities as their older counterparts.

Most industrial processes can be improved by reducing the negative effects of friction and the forces experienced which have generally led to reduced efficiency. This reduction in efficiency has large economic repercussions in most instances, and has been sought to be reduced and controlled since the industrial revolution. A prime example of undesired efficiency losses can be seen in automobiles. The friction experienced between the piston and piston sleeves causes increased fuel consumption, wear in the assembly, and eventual loss of engine compression resulting in a complete rebuild or replacement. The way in which friction is reduced is by use of an applied oil film separating the piston and sleeve.

In machining a source of friction is the interaction between the cutting tool and the chip. By reducing this undesired force there can be a substantial increase in the efficiency of the process. Less loading on the cutting tools corresponds to less material

required in the manufacture of the tool, a more efficient use of cutting fluids, as well as smaller drive systems and power requirements for the machine tool.

### 1.1 Metal Cutting Basics

There are four basic cutting operations; shaping, turning, milling, and drilling, shown in Figure 1.1 below.

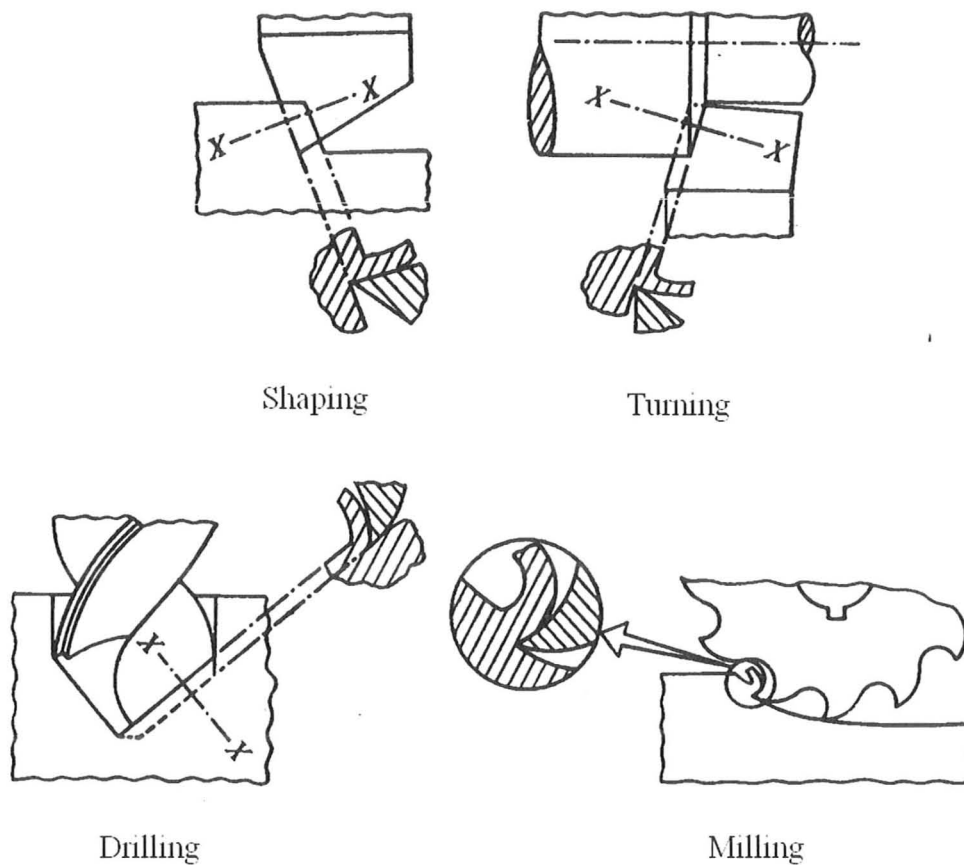


Figure 1.1 Basic Metal Cutting Operations Showing Chip Formation [1]

Looking at the appropriate sections (X-X) in Figure 1.1, it can be seen the chip formation and cutting processes are geometrically similar regardless of the operation, and

can be reduced to a simple two dimensional form as seen in Figure 1.2, known as orthogonal cutting.

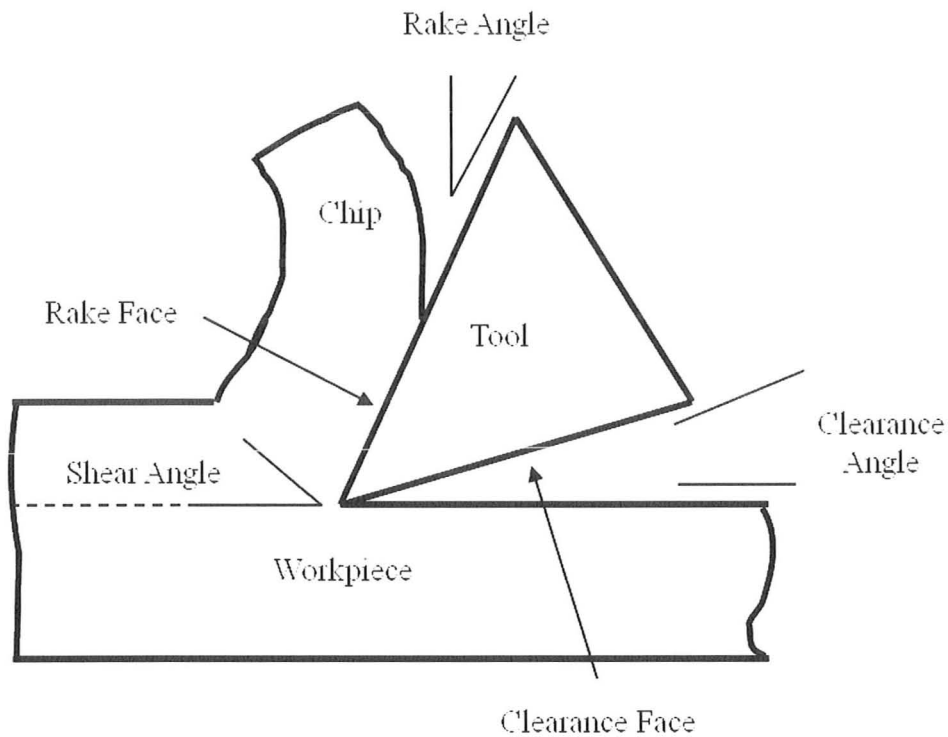


Figure 1.2. Geometry of Orthogonal Cutting

As the geometry of the cutting process and tools is similar regardless of the process, enhancements to one process can generally be extended to others, as long as cutting parameters such as cutting speed, uncut chip thickness, lubrication, etc are held similar.

In cutting operations, there are two zones of deformation, the shear and friction zones that influence the cutting response, as shown in Figure 1.3. The shear (primary deformation) zone is where the work material plastically deforms along the shear plane in

either a continuous or discontinuous fashion. The friction (secondary deformation) zone is where the chip moves over the rake face of the tool, resulting in the highest temperature in the cutting tool due to the friction between the chip and the tool. This friction and heat generation negatively impacts the cutting process, leading to increased loading and tool wear.

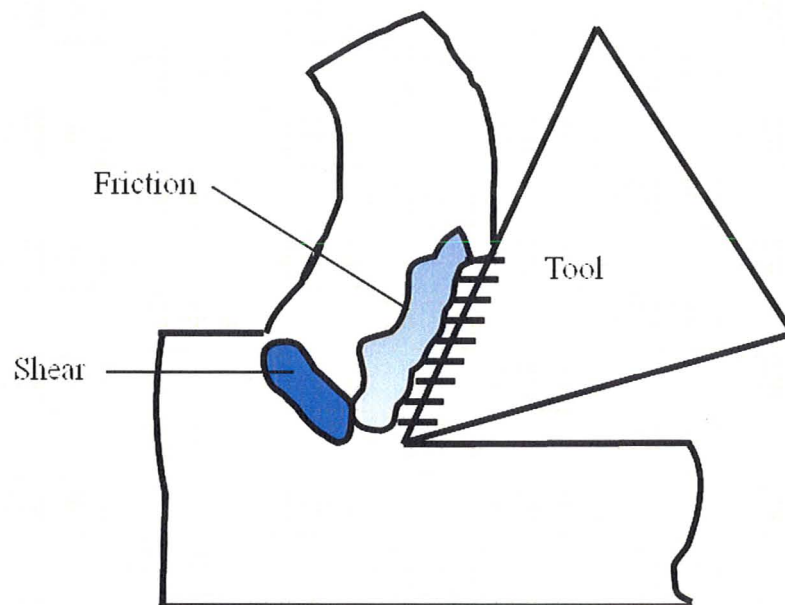


Figure 1.3. Deformation Zones in Cutting

The maximum temperature in the secondary deformation zone can be quite high, in the range of 1000 °C as it moves over the rake face, depending on the work and tool materials and cutting conditions [1]. The high temperature on the tool rake face can lead to softening of the tool material, and affects machining productivity, and dimensional accuracy and tolerances of the machined part [2]. For a general perspective, high speed steel starts to soften at approximately 550 °C. As such the cutting tool temperature must

therefore be moderated and controlled. The forces experienced in the friction and shear zones can also be quite significant, influencing the cutting process and chip formation.

The friction in the secondary deformation zone further influences and chip formation at the shear zone. Two models are generally accepted in showing the influence of the friction zone on the shear zone: the Lee and Shafer Shear Angle Solution and Merchants Shear Angle Solution. If  $\varphi$  is the shear angle,  $\beta$  is the friction angle (as defined in Figure 1.4), and  $\alpha$  is the tool rake angle (Figure 1.4), the following shear angle solutions show the relation between friction angle and shear angle;

Merchants Shear Angle Solution

$$2\varphi + \beta - \alpha = 90^\circ \quad (1.1)$$

Lee and Shaffer Shear Angle Solution

$$\varphi + \beta - \alpha = 45^\circ \quad (1.2)$$

By changing the friction angle  $\beta$  at a constant rake angle  $\alpha$ , the direct influence on  $\varphi$  can be seen. The shear angle  $\varphi$  influences the force required to shear the chip as seen in the following equation, where  $F_s$  is the shear force,  $\tau$  is the shear strength of the workpiece material,  $t$  is the thickness of material being cut and  $b$  is the width of the cut ;

$$F_s = \frac{\tau b t}{\sin \varphi} \quad (1.3)$$

A decrease in  $\beta$  causes an increase in  $\varphi$  and a corresponding decrease in the shear

force required to form the chip.

The relation between  $\phi$ ,  $\beta$ ,  $\alpha$  and the forces acting on the tool can be seen in the free-body diagram of the chip in Figure 1.4 below, where  $F_s$  and  $N_s$  is the forces acting parallel and perpendicular on the shear plane,  $F_c$  and  $N_c$  are the forces acting parallel and perpendicular to the tool rake face,  $F_p$  and  $F_q$  are the cutting and feed forces respectively, and  $R$  is the resultant force acting between the tool and chip;

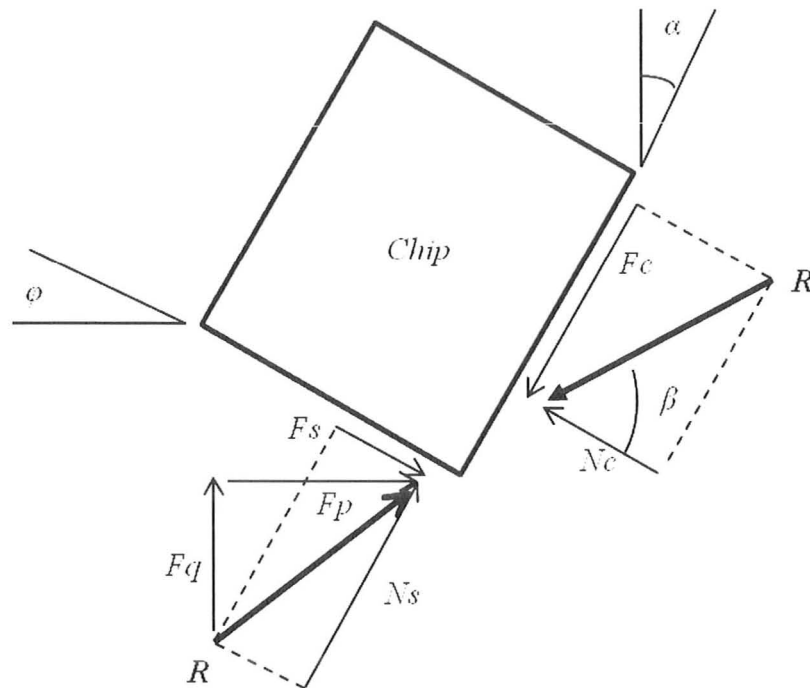


Figure 1.4. Free Body Diagram of Chip

The friction angle  $\beta$  is related to the forces acting parallel and normal to the tool rake face,  $F_c$  and  $N_c$  respectively, and is given by the following equation;

$$\beta = \tan^{-1}(F_c / N_c) \quad (1.4)$$

Representing the forces acting on the chip in the form of a Merchant's circle diagram (Figure 1.5), the relation between forces acting on the tool rake face,  $F_c$  and  $N_c$ , and the feed and cutting force,  $F_q$  and  $F_p$  respectively, can be determined.

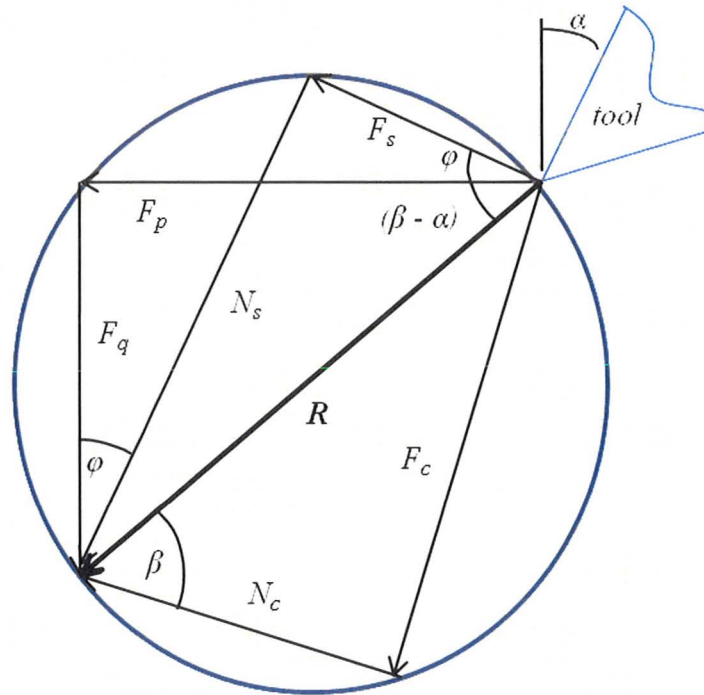


Figure 1.5. Merchant's Circle Diagram

$\beta$  can be related to the feed force,  $F_q$ , and cutting force  $F_p$  as seen below:

$$\tan(\beta - \alpha) = \frac{F_q}{F_p} \quad (1.5)$$

A decrease in tool face friction leads to a decrease in the energy required for chip formation, thus improving the efficiency of the process.

## 1.2 Friction in Cutting

Friction is the force opposing sliding motion of surfaces in contact. Classical friction theory gives the coefficient of friction as the ratio of the tangential force and normal force between the surfaces in contact. In classical friction applications due to the moderate normal forces, contact occurs at only a very few asperities between the opposing surfaces, and as such the real area of contact is actually far less than the apparent surface area. Thus the apparent area of contact does not affect the coefficient of friction. Figure 1.6 shows a representation of two surfaces in contact under similar conditions, where  $P$  is the normal load and  $F$  is the friction force.

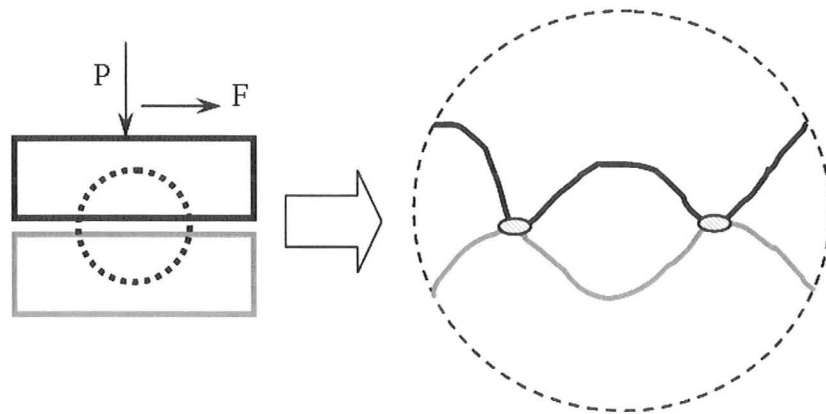


Figure 1.6. Localized Contact of Asperities

In metal cutting this frictional force opposes the motion of the chip on the tool rake face, accounting for approximately 25% of the specific cutting energy [1]. This leads to high tool temperatures that limit process productivity.

This friction force and high temperatures encountered due to friction causes several types of tool wear. Crater wear is experienced on the rake face of the tool. This wear can cause catastrophic failure on the tool as it can lead to fracture of the tool tip if much material is worn away, which increases with temperature and friction. Adhesion also occurs at the chip to tool interface due to the high pressure and temperature at junctions of the asperities in contact, which can adhere to the tool and subsequently fracture removing bits of the tool and hardened chip. These hard pieces of metal can then cause abrasive wear on the tool as they are embedded in the chip and moved along the rake face wearing away the tool. Diffusion occurs between tool and chip, which increases exponentially with temperature. Diffusion refers to atoms moving from high concentration to low concentration, from the tool to chip and chip to tool, causing a change in tool composition and reduction in hardness [1]. As such reducing friction forces experienced would improve not only tool life resulting in savings in tool costs but also reduce tool changeovers thus improving productivity.

### **1.3 Friction Reduction**

Surfaces in sliding contact can be tailored to reduce friction with several methods. A popular method is to use coatings, such as non stick coatings used on frying pans, or coatings with low shear strength used on tool surfaces such as drill bits that promote sliding between surfaces in contact by reducing adhesion. Another popular method is by using liquid and solid lubricants, such as oil and graphite.

### *1.3.1 Coatings*

Coatings have been used to improve frictional properties, spurred on by the development of new types of coatings and the recognition of how surface properties affect wear. Coatings help reduce adhesion at the chip-tool interface and chemical interactions between chip and tool, improving tool life, and in some cases reducing cutting forces, however the primary result is improved tool life. Metal cutting speeds can be governed by the temperature at which the tool starts to disintegrate, which can be increased by the use of coatings. It is estimated that approximately 20% of the heat generated during cutting is transported into the tool [3], as such improving the thermal properties of the tool can also improve tool life. Successful coatings must lower adhesion to the workpiece material, have good abrasive wear resistance and high chemical stability. These coatings influence the chip flow and formation allowing for cutting at higher speeds. The coatings should be optimized for a specific process, and have been shown to increase tool life by more than 10 times when optimized for the specific cutting condition [3].

### *1.3.2 Cutting Fluids*

Cutting fluids are generally used to offset some of the negative effects associated with friction in cutting. There are two types of cutting fluids, lubricants and coolants. Lubricants are primarily used for friction reduction at low cutting speeds with minimal cooling capacity whereas coolants are used at higher cutting speeds for heat control, with minimal friction reducing properties.

In conventional metal cutting, friction cannot be greatly reduced by the application of coolants, however the heat generated between the tool and material being machined by friction can be reduced by introduction of a lubricant. Coolants work primarily at higher speeds to cool the workpiece and tool to increase tool life. Dimensional accuracy of the workpiece and tool hardness is maintained by the removal of the heat generated during the process. Coolants are sufficiently stable as to not chemically breakdown due to the high temperatures experienced.

Lubricants work by chemically reacting with the fresh surface of the chip created during machining, forming a film of low shear stress separating the chip and the tool. Lubricants are primarily effective at low speeds for friction reduction and tend to break down during high speed operations due to heat generation. Lubricants can reduce the forces experienced thus allowing work on less powerful machine tools with less energy used and less tool failure. Temperature has a large effect on the effectiveness of the lubricant being used. Lubricants can provide a solid film protection until the temperature increases sufficiently that the film melts and breakdowns completely decreasing the effect of the lubricant [5].

Oils adhere better and react under high pressures than water based lubricants and therefore offer better lubricity [5]. Surfaces in contact can be adapted for lubricants, such as in journal bearings to optimize the process by minimizing the amount of lubricants used while relating to the smallest possible frictional force.

### **1.4 Scope and Organization of Project**

This thesis focused on improving lubrication at the chip-tool interface in metal cutting for improved frictional behavior. The innovative approach adopted was to appropriately texture the rake face of the tool using the electrical discharge machining (EDM) process. The motivation for using EDM was to create an isotropic texture that facilitates both the penetration and retention of lubricant in the tool-chip interface thus reducing the friction in cutting.

A comprehensive literature review is presented in Chapter 2. The experimental procedures are outlined in Chapter 3. Chapter 4 discusses results of the experimental work that was carried out to characterize the effectiveness of the EDM texturing process in reducing forces. Experiments referred to continuous and interrupted cutting with reference to cutting parameters as well as EDM parameters used to texture the tool. Chapter 5 includes conclusions derived and recommendations for future work.

## Chapter 2

### Literature Review

There are several current and relevant technologies that are applicable to the topic of enhancing lubrication in tribological systems. These will be discussed in this chapter along with the method by which lubricants work to reduce friction.

#### 2.1 Lubrication in Metal Cutting

The action of lubricants in reducing the frictional effects in metal cutting was first published in as early as 1881, when Mallock [6] mentioned in his paper *The Action of Cutting Tools* the following statement; “Lubricants seem to act by lessening the friction between the face of the tool and the shaving, and the difficulty is to see how the lubricant can get there, since the only apparent way is round the edge of the tool, and there it might be expected that the contact between the tool and the substance would be too close to admit of its passage. Somehow or other, how-ever, some of the lubricant does find its way between the shaving and the tool, and perhaps also into the substance of the shaving”. Mallock realized the effect of lubricants in reducing friction in metal cutting, however the mechanism by which lubricant penetration was realized was unknown to him at that time.

### 2.1.1 How Lubricants Work

Considering two surfaces in contact as shown in

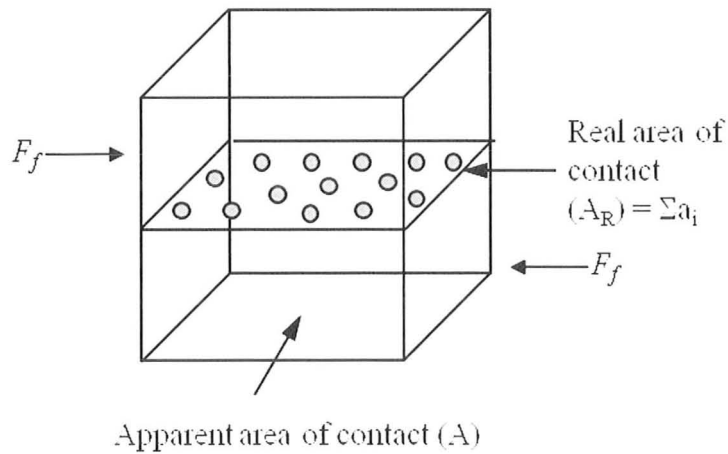


Figure 2.1, the real area of contact  $A_R$  is a summation of the individual areas associated with asperities in contact, which is significantly less than the apparent area of the surfaces. The friction force  $F_f$  is simply the force required to shear these asperities at their contacts and is a function of the real area in contact and shear strength of the weaker material  $\tau$ , as shown in equation (2.1).

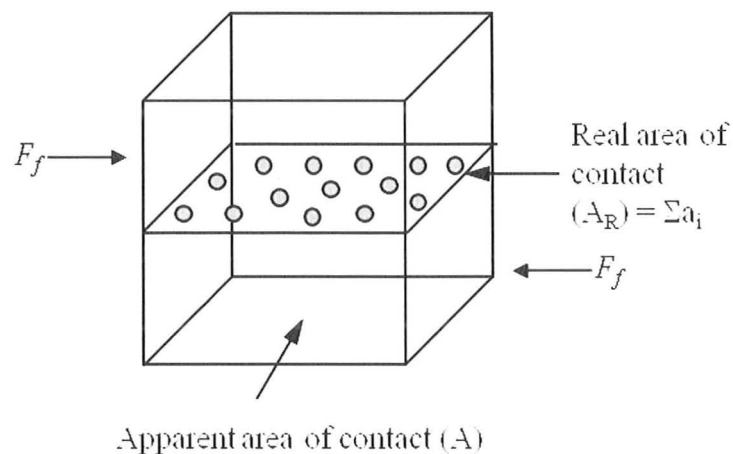


Figure 2.1. Real and Apparent Contact

$$F_f = A_R \tau \quad (2.1)$$

On application, lubricants can penetrate through the gaps between asperities, and under the pressure experienced can react chemically with the metal substrates to form a solid film. The normal contact pressure is now supported by both the base materials and the solid lubricant film as represented in Figure 2.2.

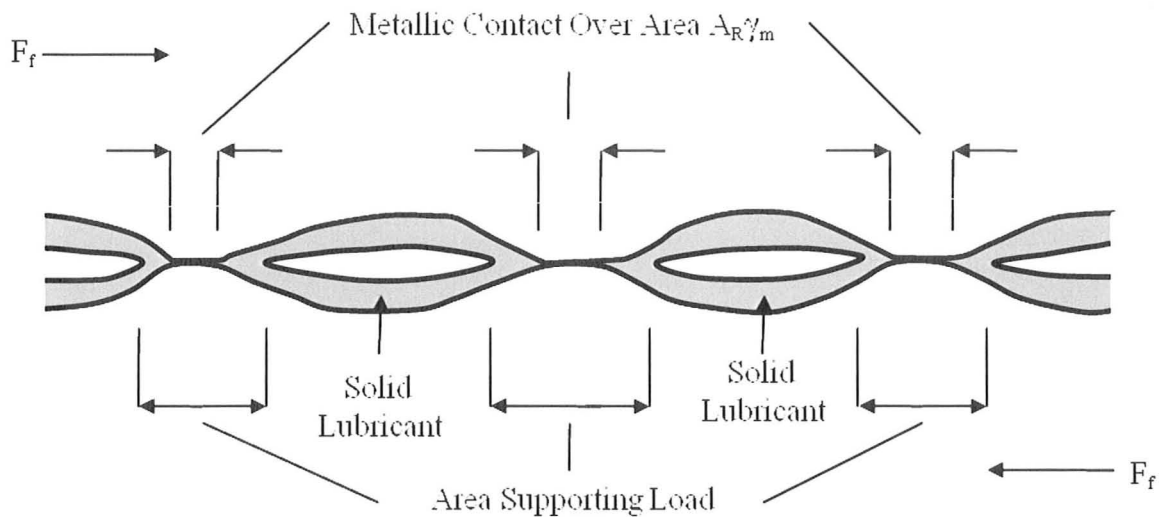


Figure 2.2. Sliding Between Surfaces with Solid Lubricant Layer

The force required to shear the two surfaces is therefore now a function of the real area in contact, and shear strength of the weaker material and lubricant. If  $\gamma_m$  is the proportion of this area over which metallic contact occurs, and  $\tau_1$  and  $\tau_2$  are the shear strengths of the softer metal and softer lubricant layer respectively, the friction force is given as;

$$F_f = A_r [\gamma_m \tau_1 + (1 - \gamma_m) \tau_2] \quad (2.2)$$

By introducing a lubricant, the solid film that forms reduces the metallic contact  $\gamma_m$ , as the film now supports some of the load. If the film has a lower shear stress ( $\tau_2$ ) than the base material ( $\tau_1$ ), the friction force is now reduced. It should be noted that lubricants that reduce friction when machining one material may increase friction when used on another. If the lubricants used were not chemically reactive with the formed chip no solid lubricant film may be formed. Thus the metallic contact  $\gamma_m$  equals unity and the load is supported entirely by the base material. Negative lubrication can also be found due to exclusion of oxygen which can act as a lubricant by reacting with the new surface. An oxide that forms may have weaker shear strength than workpiece material, thus acting as a lubricant by reducing metallic contact [7].

In metal cutting however, the normal stresses experienced on the tool rake face can be high enough that the real area of contact approaches the apparent area of contact. No lubricant would be able to penetrate into the interface in this region as the asperities are plastically deformed significantly enough that no gaps exist for lubricant ingress. This was mentioned by Mallock [6] when pondering the mechanism of lubricant penetration.

The stress distribution in machining can be measured using a split tool technique. A split tool is made of two segments (Figure 2.3) separated by a gap that is small enough to prevent extrusion of chip material but large enough to render them independent of each other.

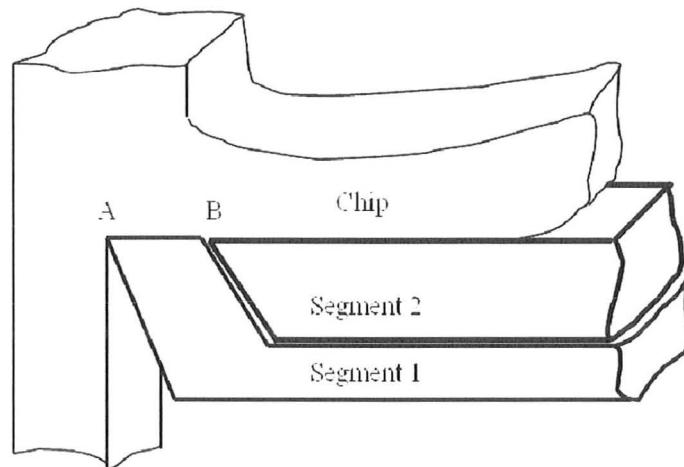


Figure 2.3. Split Tool to Measure Cutting Forces

Segment 1 is connected to a dynamometer to measure the two components of the cutting force. By systematically changing the length AB of segment 1, usually by grinding away the clearance face, the normal and shear forces for various distances AB from the cutting edge per unit width are measured to calculate the distribution of normal and shear stress experienced by the tool.

What has been determined by utilizing the split tool technique is there are two separate regions on the tool face as shown in Figure 2.4, the sticking and sliding zones. The sticking zone is characterized by high normal stress, as high as 3.5 GPa [1]. In this zone the surfaces plastically deform to such an extent that the area in contact between the chip and tool at the interface equals the apparent area. The shear stress experienced is that of the shear stress of the work material. The sliding zone is characterized by lower normal stress. The shear stress becomes a function of a constant coefficient of friction, and the total area in contact is less than the apparent area allowing for lubricant

penetration. It was found there is a sharp divide between the zone of sliding and sticking [8].

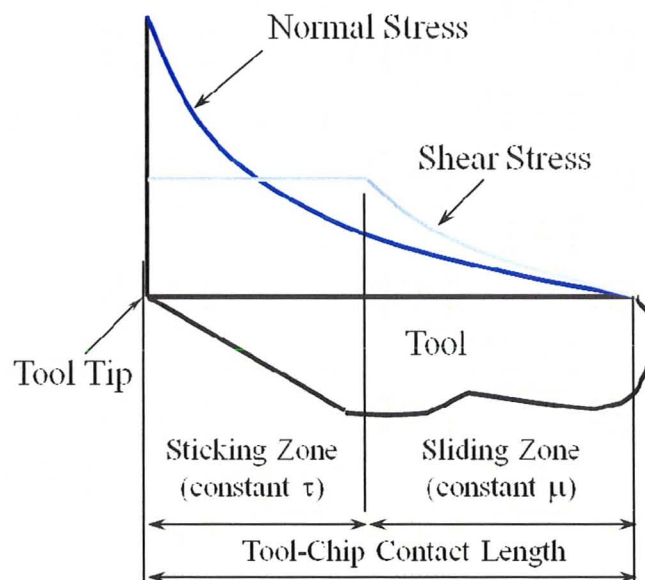


Figure 2.4. Stress Distribution on Rake Face of Cutting Tool

It has been experimentally determined by Childs [9] that lubrication is only possible in the sliding zone as lubricants are unable to penetrate the sticking zone.

If lubricant can penetrate into the chip-tool contact area in the sliding zone it can decrease the cutting forces experienced and reduce the contact length between chip and tool, improving the surface finish and reduce formation of the built up edge [10]. Lubricant penetration is an effect then of the asperities in contact, penetrating through micro channels by capillary action. These channels for fluid penetration have been found to be anywhere from one micrometer to one chip thickness long and to be dependent on

the normal stress distribution and surface irregularities between chip and tool [11][7].

Referring to Figure 2.5 the lubricant penetration can be seen into the sliding zone over a penetration length  $L$ .

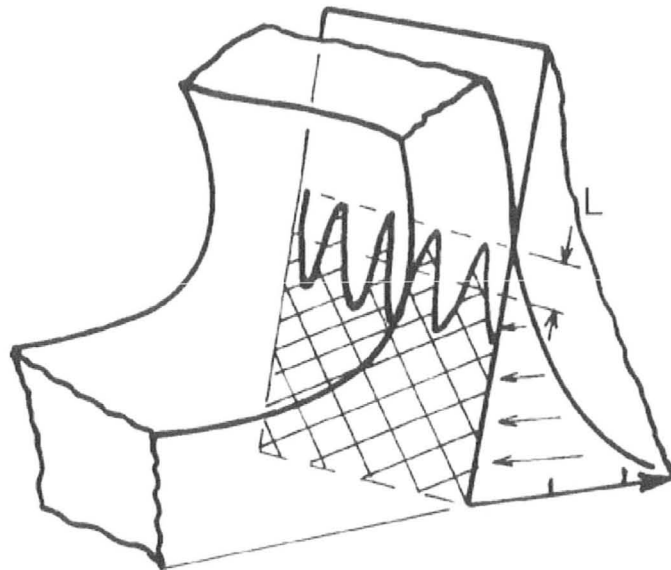


Figure 2.5. Fluid Penetration Through Micro Channels of Length  $L$  at Interface [9]

It was found that only milliseconds were required for fluid penetration into the sliding zone through capillary action [12]. Penetration of the lubricant can be partially improved by increasing the pressure driving the lubricant into and through the micro channels, and will be discussed in the following section.

### *2.1.2 Application of Lubricants*

The mode of application of lubricant is important in determining the volume of lubricant that could potentially penetrate the sliding zone. The conventional way of

application is flooding of lubricants, which requires large volumes of lubricant used compared to the area being cut [10], which may be completely unnecessary. For instance cutting tests carried out at Warwick University [10] mentioned no change in roughness of the surface finish of a machined workpiece using reduced lubrication compared to conventional flood lubrication. When the lubricant was applied in drops with a hypodermic needle, the surface roughness was found to be similar to when lubricated as a flood. Substantial reductions in rake face friction can result from relatively modest penetration of the lubricant into the interface, which implies that the volume of lubricant may be minimized without comprising performance [13].

It should also be noted there is a difference in the effectiveness of lubrication between continuous cutting operations such as turning and interrupted operations such as milling. In continuous cutting the lubricant is being continually wiped away and there is a balance between machining pressure removing the lubricant and lubricant pressure introducing the lubricant [9]. In interrupted cutting lubricants have better periodic access to the complete tool face, and are continually replenished.

De Chiffre [14] conducted a turning test using carbon tetrachloride vapor as a lubricant, reducing the coefficient of friction from 0.5 to 0.25 when using the lubricant as opposed to a dry cutting tool. A balance existed between vapor pressure and machining pressure, and there existed a maximum vapor pressure past which no improvements could be found.

Lubrication models indicate that the rate controlling step in lubrication is the transport of the lubricant molecules into the tool chip region, as opposed to the rate of chemical reaction between the lubricant and chip [7][15]. Experiments conducted by Shirakashi [15] with a vapor lubricant tetra chloromethane at various vapor pressures and cutting speeds ranging from 1.5 to 105 mm/s found that the coefficient of friction decreased with increasing vapor pressure similar to work by De Chiffre [14], as the ability of the lubricant to penetrate the interface increased with pressure. Full lubrication was achieved when the rate of transportation into the interface was equal to the rate of consumption, at which point no further improvements could be realized.

### *2.1.3 Effect of Cutting Parameters*

Unfortunately the effectiveness of lubricants in reducing forces is also limited by the cutting parameters. It has been found when using carbon tetrachloride in a copper turning operation that at low cutting speeds lubricants are effective at reducing the cutting forces, as reported by Childs [9]. Childs determined that at low speeds lubricants help moderate the effect of the rake face adhesion between the chip and the tool, and with the proper lubricant for the material being cut boundary lubrication can be realized [7]. The results can be seen in Figure 2.6 which outlines the effectiveness of lubricated cutting compared to dry cutting as a function of cutting speed. The effectiveness of the lubricant is greatly reduced as cutting speed increases to a point where all effectiveness of lubricant is lost.

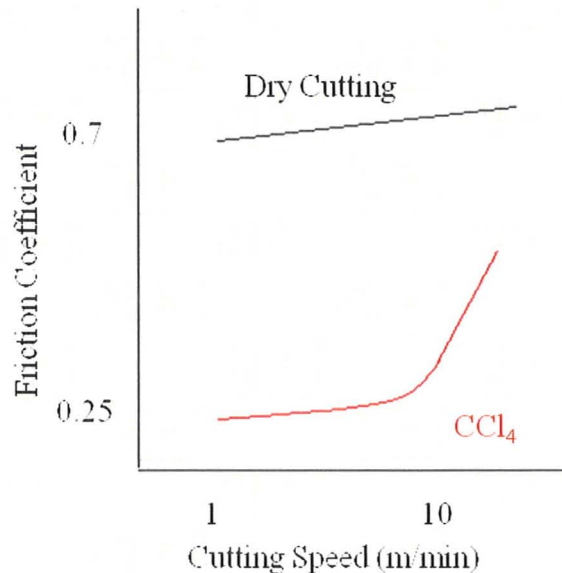


Figure 2.6. Effect of Carbon Tetrachloride as a Lubricant in a Copper Turning Experiment [9]

At low cutting speeds, typically less than 10 m/min, the effectiveness of the lubricant in reducing friction was considerably more than at higher speeds. At a cutting speed of approximately 30 m/min the friction of the lubricated tool approached that of the non lubricated tool and the lubricant lost all effectiveness [9]. Any lubricant action would be reduced by an increase in cutting speed which will reduce the rate of lubricant access and the reaction time between the lubricant and the metal chip. The influence of interface temperature with cutting speed can also lead to the breakdown of the lubricant, thus affecting its function.

The effects of cutting speed become more pronounced as the uncut chip thickness increases. Childs [9] found that lubrication was possible only over a range of cutting speeds and uncut chip thickness, which decreased with increasing uncut chip thickness as

seen in Figure 2.7. Increasing the uncut chip thickness increases the length of the path down which the lubricant molecules must travel, thus reducing effectiveness at a given speed and reducing the speed range over which lubrication is possible [13].

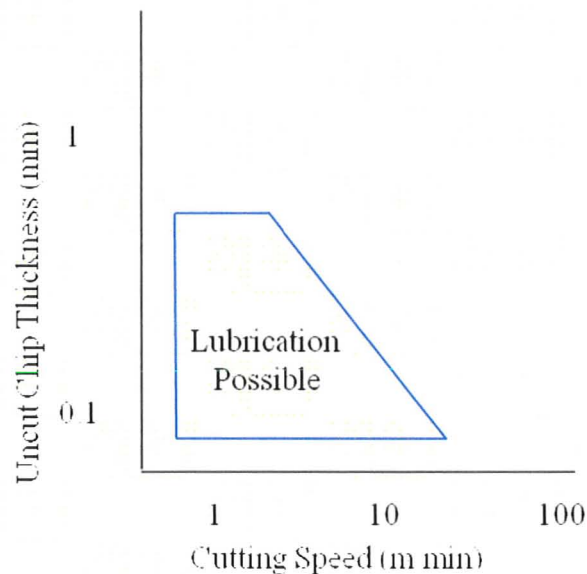


Figure 2.7 Lubrication Range as a Function of Uncut Chip Thickness and Cutting Speed [9].

Due to the surface roughness and light loading in the sliding zone, the real area in contact is less than the nominal area, as such lubricant penetration is possible through micro channels and capillary action at this interface [9][11][13]. It was determined by Childs [9] that even at extremely low cutting speeds, around 0.25 mm/min tested, that lubricant never penetrated into the sticking zone [10][9].

It is clear that lubricants are effective only at low cutting speeds on the order of only a few tens of meters per minute. These speeds correspond to operations such as broaching, threading and shaping where the cutting speeds are on the order of 10 m/min

or less, significantly less than cutting speeds used in processes such as milling and turning wherein cutting speeds are on the order of several hundred meters per minute [16][17][18]. Broaching operations are common in industries such as aerospace for machining internal gears or splined shafts in difficult to machine aerospace alloys, where cutting forces experienced can be quite significant. Improved lubrication would be of significance in these operations, and it will be such low-speed processes that can benefit the most from enhanced lubrication.

#### *2.1.4 Dependence on Asperity Contact for Lubrication*

Lubrication is only accessible to the sliding zone through capillary action. The asperity contact not only creates micro channels for the lubricant to flow, but also influences chemical reaction between lubricant and metal substrates. It was found in tests by Shirakashi [15] that the reactivity between lubricant and metal substrate increases with pressure. Average normal stress increases with spacing of asperities of two surfaces in contact, thus with increased roughness and pressure, which is similar to observations made by Childs [9] that controlled roughness is significant in enhancing lubrication.

Carbon tetrachloride used in most literature is an excellent lubricant and can provide significant reductions in friction. Unfortunately it is toxic and thus not practical in industrial applications, and only used for testing purposes. Most industrial lubricants are not as effective thus the range of effectiveness is more limited, and methods to improve the application of practical lubricants is needed.

## 2.2 Engineered Surfaces

Surfaces can be engineered to have a specific texture to optimize the effectiveness of lubrication. Surface texturing is an idea that has been applied to bearing and automotive applications already. Used in piston ring assemblies, texturing allows engine systems to operate with lower viscosity oil. Texturing is also used in bearings, seals, etc to act not only as a lubricant reservoir, but also to trap debris that can disrupt and breakdown the tribological system by interfering with the relative motion of the surfaces [19].

Two types of surface textures have been reported in the literature recently: dimpled textures and linear textures.

### 2.2.1 *Dimpled Textures*

Dimpled texturing refers to a pattern of dimples of a given size and spacing on the face of an object, to aid in lubricant penetration and retention.

For textured surfaces, small cavities or dimples uniformly distributed over the sliding surface have been found to have the best tribological effect, which serve the function of a series of small micro bearings, each acting as a reservoir. In gears and pistons rings, as the contact pressures experienced are extremely high, hydrodynamic equations predict that the film thickness in these instances is too small to prevent the contact of opposing asperities, much like in metal cutting operations. However in reality this has been found to be not the case, and thick films are present. This is due to the variation of viscosity with high pressure and elastic deformation of the bearing surfaces

and the surface roughness. These results indicate that even if it is numerically predicted that no fluid film will be present between the chip and tool in metal removal operations, there may still be a film that can beneficially influence the process.

Kovalchenko [20] tested disks textured with dimples that maintained hydrodynamic lubrication even with increasing loads, from 0.16 to 1.6 MPa. He found that higher viscosity oil caused increased friction compared to lower viscosity oil. Approximately 50% reduction in friction was found, generally at all speeds used (0.15 to 0.75 m/s). This experiment involved no plastic deformation and the stresses were insignificant compared to machining. An example of a dimpled surface can be seen in Figure 2.8.

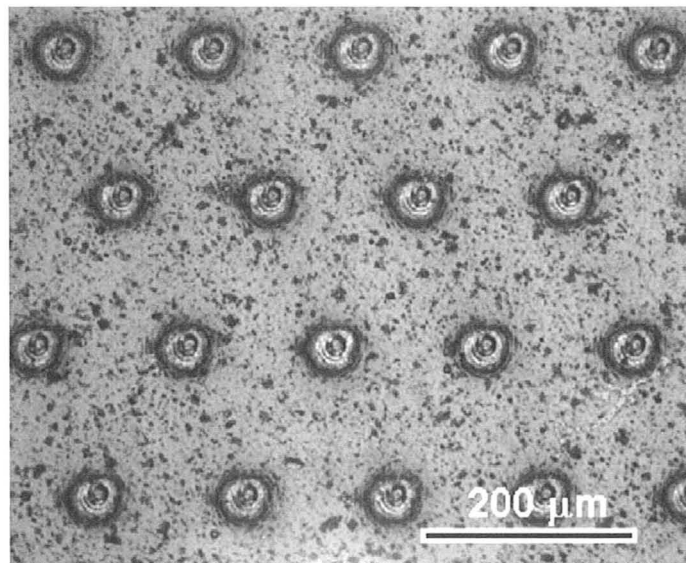


Figure 2.8 Representative Dimpled Texture [28].

Ryk [22] tested dimpled surfaces on automotive components, with dimples of

diameter 100 micrometer and depth 10 micrometer, and a textured area density of 13%. Even in lubricant starved conditions there existed a reduction in the frictional force, as the textures were able to retain lubricants and wear particles. When tested on piston rings there was a reduction in friction of up to 25% at normal speed applications, however an optimum speed was required for the maximum benefit of a 30% to 40% reduction in friction.

Ryk [22] tested several dimple depths and found that an optimum dimple depth existed, and that dimples deeper than the optimum were detrimental in maintaining hydrodynamic pressure. There was an optimum oil viscosity and dimple depth that could yield maximum friction reduction, which is similar to work by Kovalchenko [20] who found an optimum oil viscosity. Ryk found that the actual shape of the micro dimples did not play a role and the most significant parameter for optimum load capacity was the ratio of dimple depth to diameter.

Vihena [23] investigated textured and non-textured steel samples, testing with a reciprocating pin against a stationary disc using samples that were textured with a dimple density of 6.7% and 26.8%. At a constant load on a pin on disk test with variation of speeds between 0.01 and 0.12 m/s, he demonstrated that the textured samples provided 10% less friction than the non-textured surfaces.

Etsion [24] conducted a ball on disk test using textured disks and found that the lifetime of the textured sample disks could be similar in magnitude to using coatings and as much as eight times longer than that of non-textured samples [3], due to the improved

lubrication provided by the textures and the ability to trap wear particles. The shape of the dimples was again found to not play a significant role, with the most significant parameter being the ratio of depth to diameter of the dimples [24].

Zhu [25] used micro dimples on the surface of a chrome coated iron substrate. The dimples tested were 240 micrometers in diameter, and varied in depth from 4 to 22 micrometers. The sliding contact zone was soaked in diesel oil to act as a lubricant. An optimum dimple depth of 10 micrometers was found, leading to a reduction in frictional forces by up to 30%.

Qian [26] tested micro dimples also on a chrome coated surface. A micro dimple array with hundreds of micrometers in diameter and several micrometers in depth were produced, and again a reduction of friction on the order of 30% was feasible with textured surfaces. Deeper dimples provided greater reduction in the coefficient of friction, which is counter to some of the previously mentioned experiments, however this still leads to the suggestion that there is an optimum depth and diameter of dimples for specific operating conditions for optimal friction reduction.

It was found by Galda [27] when using a bronze block contacting a steel rotating ring that the surface texturing of the block with an area density between 20% and 26% resulted in significant improvement in wear resistance. Spherical shaped dimples were found to be better than drop shaped dimples with regards to wear resistance, and there was an optimum dimple area ratio and shape that provided maximum force reduction. This is counter to experiments by Etsion [24] who determined the shape of dimples was

not important. It is more likely that specific shapes may better suited to certain operating conditions.

As mentioned, dimple depth and diameter, speed, load, and oil viscosity all have an effect on friction reduction. Galda [27] looked at the effect of surface roughness on Stribeck curves. Stribeck found the possibility of a point of minimum friction with respect to journal bearings and load and speed characteristics. Stribeck curve shows friction varying with velocity and load, as seen in characteristic Stribeck curves such as that in Figure 2.9. The graphs are based on several regions based on the speed and load characteristics. With a low speed or high loads the bearings experience boundary lubrication. With increasing speed or decreasing load mixed lubrication is experienced where the interface constitutes some points of surfaces in contact and some areas separated by fluid. At high speeds or low loads fluid film lubrications is experienced where the surfaces are completely separated by a fluid.

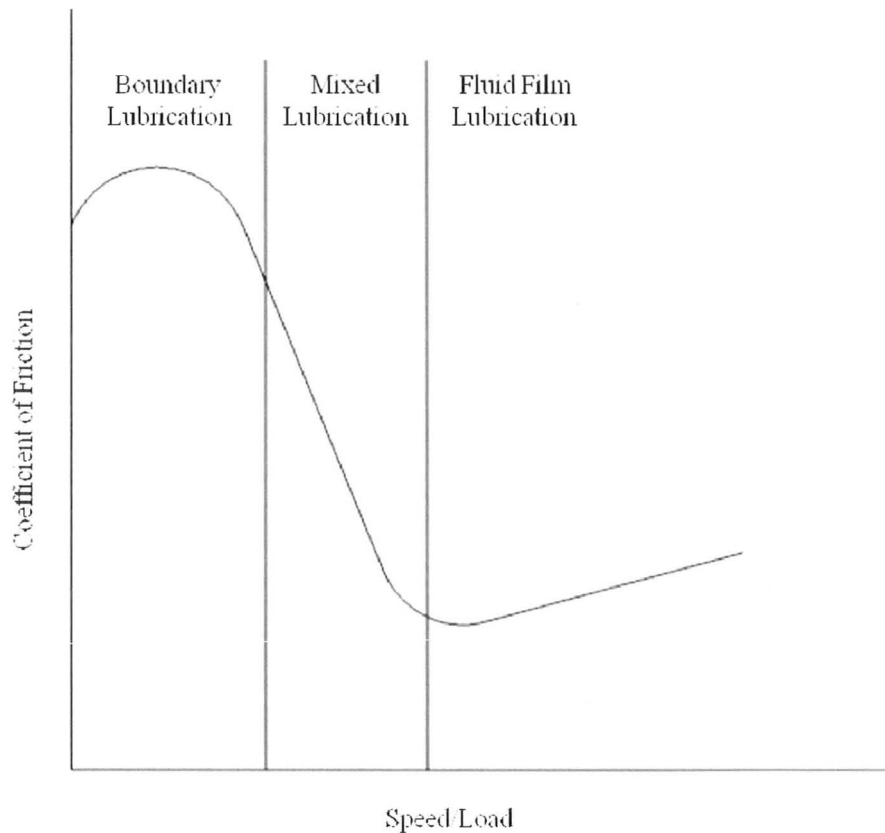


Figure 2.9. Characteristic Stribeck Diagram

Galda [27] found that surface roughness greatly influences friction on the Stribeck curve. Rough surfaces show the highest friction coefficient followed by medium and fine surfaces, however dimple textures can act as micro hydrodynamic bearings by providing lift while increasing the roughness of a surface as previously mentioned by Qian [26], Etsion[24] and Zhu [25]. Surface texturing can expand the range of hydrodynamic lubrication for high and low viscosity oil lubricants on the Stribeck curve. It should be noted that the friction reduction depends on the specific case, taking into account all

parameters such as load, speed, oil viscosity resulting in an optimum dimple or roughness configuration.

Previously mentioned research has focused on the effects of liquid lubricants, however in respect of environmental benefits the application of solid lubricants needs to be considered. Voevodin [28] applied solid lubricant of MoS<sub>2</sub> and graphite to a dimpled texture which were between 10 and 20 micrometers in diameter with depth of 3-5 micrometer, over a dimpled surface area between 0.5% to 50%. The coefficient of friction was found to be between 0.2 and 0.4 with the texturing and lubricant, compared to about 0.6 when untextured and unlubricated. There was again an optimum dimple area and size that provided the maximum reduction in coefficient of friction and provided sufficient lubricant while still supporting the pressure. Wear was considered and found that after 13,000 cycles there was still lubricant in the reservoirs, suggesting a potentially effective replacement for liquid lubricants [28].

A multilayer coating was tested by Jiang [29] on a titanium nitride substrate. The engineered coating was integrated with controlled surface roughness, similar to specific dimple sizes, to utilize the wear resistance of coatings with the benefits of an engineered surface. He found that the combination of the soft lubricating layer on an engineered hard layer can effectively reduce friction and improve wear performance increasing tool life.

A review of the literature related to the subject of dimpled textures indicates that based on application specific operating conditions such as relative velocity and load,

different dimple diameter, depth, and spacing are required for maximum friction reduction.

### 2.2.2 *Linear Textures*

In place of dimpled texturing, linear texturing can also be used in the form of fine slots or grooves across the surface. Piston surfaces in hydraulic motors were textured by Pettersson [30] who used parallel grooves and crossed grooves each of four different spacing which were tested and compared to a polished surface and a non textured sample. He found that friction levels were marginally influenced by textures however friction fluctuations were reduced. Less fluctuation in friction could be explained by the reduction in contact area between surfaces. After 1000 cycles of testing, the textured surface and polished surface had the same level of friction as the non textured samples suggesting that the texture had worn out.

Linear textured surfaces have also been used in the strip drawing process. Costa [31] conducted drawing tests at a speed of 22 mm/s with parallel groove patterns on the surface of the die, oriented parallel and perpendicular to the drawing direction. Significant reduction in friction was found with grooves perpendicular to the drawing direction.

Experiments were performed by Kawasegi [32] with cutting tools that had nanometer or micrometer scale texturing on the tool rake face, consisting of lines running parallel and perpendicular to the chip flow direction, as seen in Figure 2.10 below.

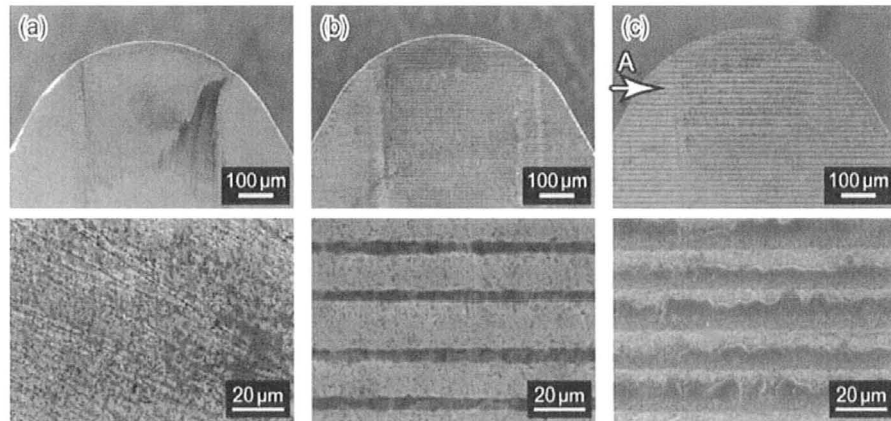


Figure 2.10. Linear Textures on Cutting Tools [32].

It was determined that significantly lower friction could be achieved when the scale of texturing was on order of nanometers rather than micrometers as seen in Figure 2.11 below.

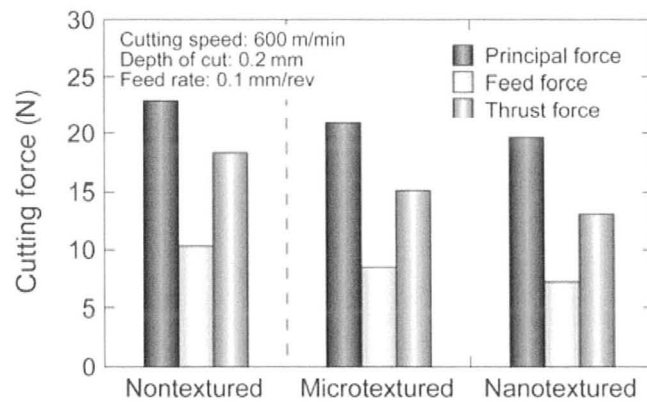


Figure 2.11. Cutting Forces Based on Scale of Texturing [32].

The reduction in friction was found to strongly depend on the direction of texture. Lower cutting forces were achieved when the texture was perpendicular to the chip flow direction rather than parallel, similar to Costa [31] who noted the same effect. Texturing

direction was also important in the amount of material that adhered to the tool face. It was found that more material adhered to the parallel texture while the perpendicular texture had minimal adhered material. The texture on the order of micrometers were also found to be filled with work material after cutting, however this was not the case with the nanometer textures. See Figure 2.12 below for a micrograph of tooling filled with work material [32]. A non-textured tool was used at cuttings speeds of 60 m/min, 300 m/min and 600 m/min in figures a) through c). Work material adhered to the rake face of the tool can be seen. Figures d) through f) represent the same cutting speeds using a nanoscale textured tool, showing less material adhesion with an increase in speed.

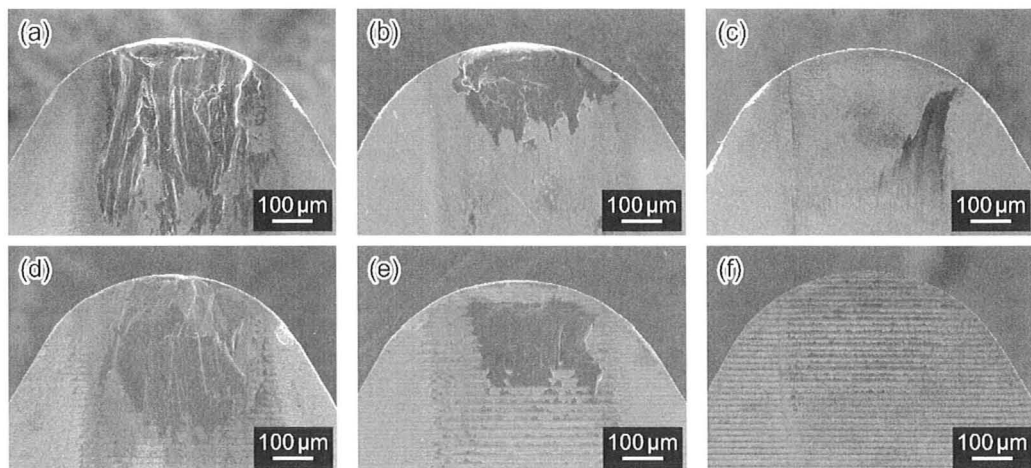


Figure 2.12. Performance of Textured Tool [32]

It was found that texturing was beneficial only above cutting speeds of 420 m/min due to adhesion of the material. At low speeds more material adhered to the tool than at high speeds. The experiments were also performed without lubrication, and a decrease in cutting forces was experienced, which suggests that the reduction in forces could be due

to thermal softening of the workpiece material rather than the texture enhancing coolant penetration.

Some materials such as aluminum alloys are easy to cut however due to high material adherability chips adhere strongly to cutting edge of tool leading to increased tool breakage. Sugihara [33] demonstrated that textures promoted anti-adhesive effects at the interface, reducing the amount of aluminum adhered. Grooves were created on the rake face of a cutting tool 100-150 nm deep spaced 700 nm apart and tested at a cutting speed of 380 m/min. The rake face of the tool was observed after cutting 1800 m of material, and found grooves parallel to the main cutting edge decreased material adherability. Compared to wet cutting, when no cutting fluid was used adhesion effects increased, thus wet cutting with the texture was superior compared to non textured and polished tools.

As a result of experiments using linear textures, it can be seen that they are effective in enhancing friction reducing properties of lubricants, however linear textures perpendicular to the sliding direction are more beneficial than those parallel to the sliding direction. Scale of the textures was also found to be important, similar to characteristic dimple size required for maximum friction reduction.

### **2.3 Texturing Processes**

There are several processes used to generate the previously mentioned textures which will be discussed in this section;

### 2.3.1 Laser Surface Texturing

Lasers machining has been the most popular method used to texture sliding surfaces for improved lubrication. Kovalchenko [20] used laser machining to texture disks with dimpled patterns and successfully improved lubrication effects in sliding tests. An example of a laser textured surface can be seen in Figure 2.13.

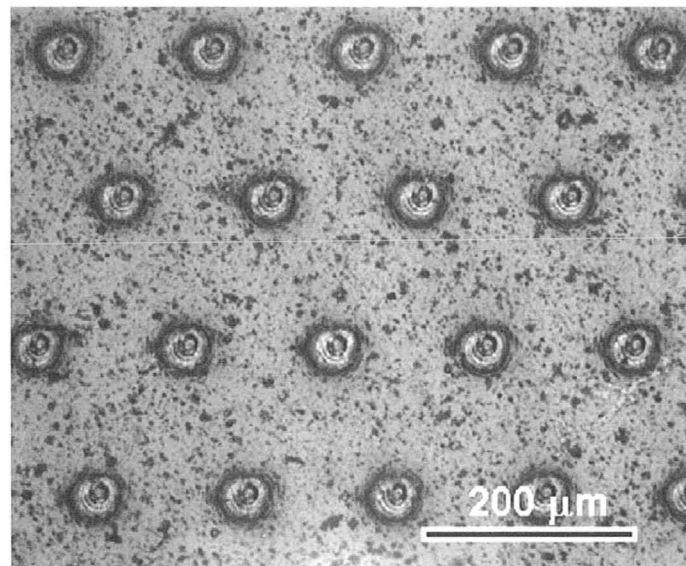


Figure 2.13 Example Laser Textured Surface [28]

Ryk [22] tested laser textured surfaces on automotive components, again finding laser surfaces could be used to improve lubrication. A UV laser beam was used to surface texture several TiCN coated cutting tools with dimple texturing by Voevodin [28] and nano/micro textured surfaces were created using femto second lasers by Sugihara [33]. Kawasegi [32] used lasers operating with femosecond pulses to create linear grooves on cutting tools. In all cases the laser textured surfaces resulted in a reduction of friction.

Etsion [24] conducted a ball on disk test using laser textured disks and found the lifetime of the textured disks to also significantly increase.

Laser machined surfaces may involve some recast material at the edges of the textures which require a secondary operation for removal similar to that experienced by Vihena [23], who used high intensity laser pulses to texture components. This can be seen in Figure 2.14. The melted material that was recast needed to be polished and removed prior to experimentation as it led to increased friction in some cases [23] [28].

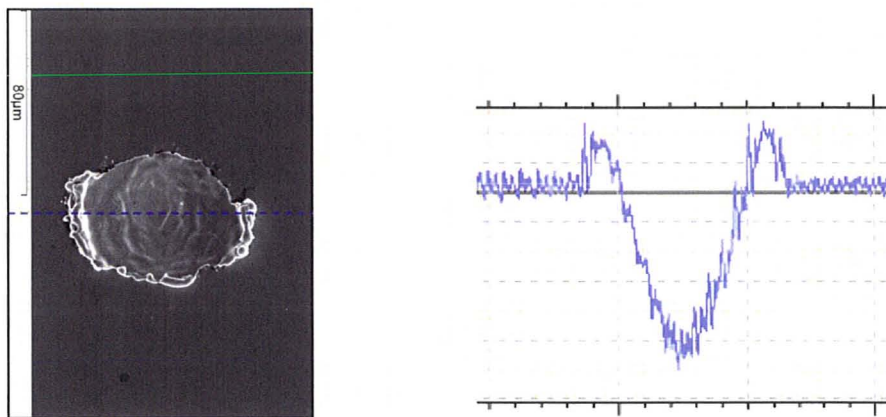


Figure 2.14. Laser Surface Dimpling and Corresponding Formtracer Profile [23]

The advantage of lasers over other types of machining is that they are environmentally clean, requiring no oils or mediums for machining, and have excellent control and precision for dimple generation. However they may have an issue with recast material as previously mentioned and require a secondary finishing operation to remove any recast prior to application.

### 2.3.2 Electrochemical Machining

Electrochemical machining (ECM) has been also used to texture surfaces in sliding contact for friction reduction. ECM works by passing a high current from a movable cathode through a electrolytic fluid to the workpiece, which is the anode from which material is removed by electrolyte dissolution .Zhu [25] used ECM to create micro dimples on the surface of a chrome coated iron substrate. Using an insulating mask coated on the surface of the test sample a dimpled pattern was created as seen in Figure 2.15, creating a test sample as seen in Figure 2.16. Dimples with a diameter of  $240\ \mu\text{m}$  were machined, ranging in depth from  $4$  to  $22\ \mu\text{m}$  resulting in a reduction in the coefficient of friction.

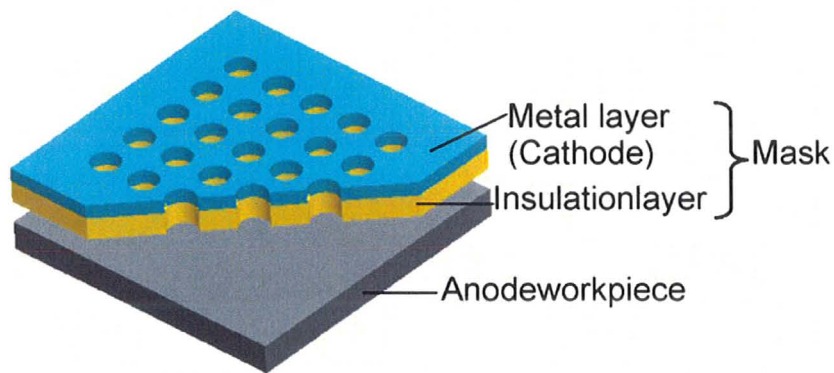


Figure 2.15 Through-Mask Electrochemical Machining [25].

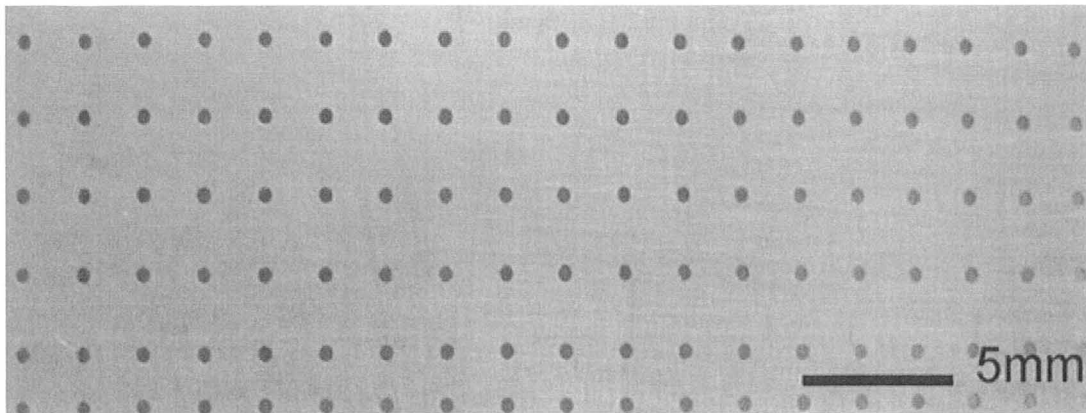


Figure 2.16. Dimpled Pattern as a Result of ECM [25].

Qian [26] performed a similar test using through mask electrochemical micromachining, again resulting in a reduction in friction. The key advantage of ECM is that no residual stress or cracks are associated with the ECM process as with process like laser machining which remove material through intense heat generation.

### 2.3.3 Other Processes

There are processes other than the two previously mentioned that can be used to texture surfaces.

Piston surfaces in hydraulic motors were textured by Pettersson [30] using embossing tools creating diamond textured surfaces of parallel and crossed grooves.

Berlet [34] noticed a correlation between grinding force and friction coefficient when testing a pin on disk test. Multiple tests were conducted using a variation of coolant composition (sulphur and phosphorous additives), contact forces, and contact time on grinding the surface of the disk. All factors influenced the coefficient of friction when

used on the pin on disk test. The result of changing these factors was a change in surface composition of the disk as well as a change in the surface topography and roughness. With optimization of these factors a disk with a specific surface topography resulted in a minimum coefficient of friction.

Franzen [35] used a rolling process to texture tooling to increase friction to influence and control material flow during deep drawing process. The textures were linear in nature and of multiple configurations. The textures were created using a CNC milling machine and a ball point tool mounted on the spindle. The textures increase the friction locally on the sheet to influence the drawing procedure.

The disadvantages of using mechanical texturing procedures as compared to a process such as laser machining or ECM are the wear on the tooling required to create the pattern causing the need for potentially complex and expensive consumables, as well as an increase in manufacturing time.

## **2.4 EDM Texturing**

Electrical Discharge Machining (EDM) can produce textures on cutting tools possibly at a higher production rate than the previously mentioned methods. EDM has been found to also be effective in reducing friction in cutting tools.

### *2.4.1 Previous Work with EDM*

Cemented carbide cutting tools were used by Jianxin [36] with micro holes created by EDM on the rake and flank face of the cutting tools, close to the cutting edge

as seen in Figure 2.17, of diameter range between 200-250 micrometers and depth of 250 micrometers. Hardened steel workpieces were used without any cutting fluids at a cutting speed of 115 m/min, with a solid lubricant of molybdenum disulfide filled in the micromoles to create a self lubricated cutting tool. The cutting forces were reduced by creating a lubricating film between tool and workpiece. After cutting a thin lubricant film was visible on the wear tract of the tool [36]. As such the possibility of using EDM in some form to texture cutting tools for friction reduction is possible, however this has not been significantly explored. EDM process can include wire and die sinking and a variety of different types of textures can be generated.

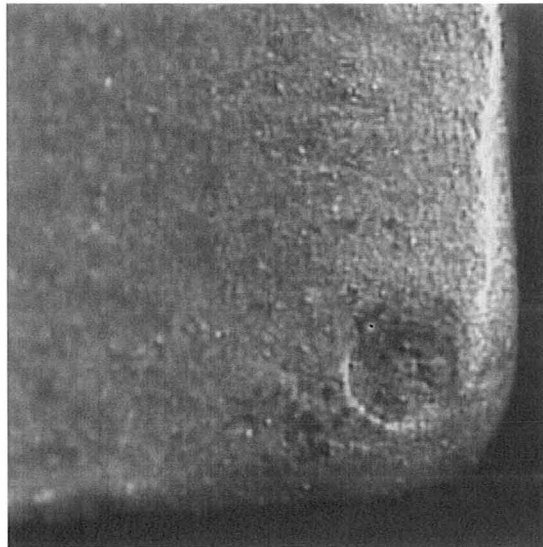


Figure 2.17 EDM Micro Hole on Rake Face of Cutting Tool [36].

#### 2.4.2 How EDM Works

EDM uses two conductive surfaces separated by a di-electric fluid for machining. One surface is the electrode, machined into the negative of the desired profile to be

created, and the other surface is the workpiece to be machined, both of which must be electrically conductive. When a voltage is applied across the surfaces the dielectric fluid breaks down and allows energy to flow through a plasma channel between surfaces. This plasma channel is extremely hot causing a crater to be melted in the workpiece and the electrode. The process can be seen in Figure 2.18 below for a single spark. The diagram shows the charged electrode, creation of plasma channel, breakdown of plasma channel when the voltage is turned off, and finally the flushing and remaining crater shape left.

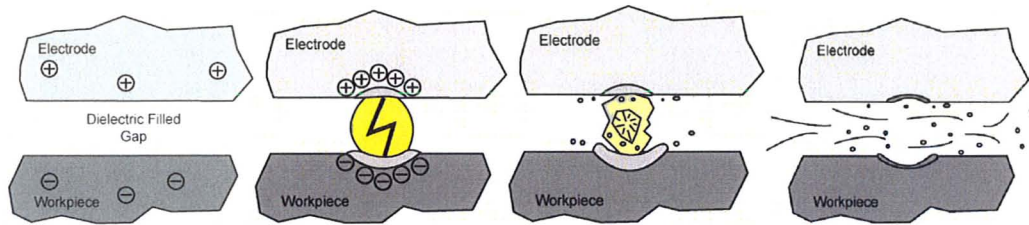


Figure 2.18. EDM Process

Millions of sparks can occur per second during EDM, texturing a surface faster than laser machining, leaving a workpieces with a crater filled surface, which are positively skewed as seen in Figure 2.19 . The positively skewed surface acts like a series of reservoirs that can retain lubricants. Each reservoir acts as a micro bearing, reducing friction.

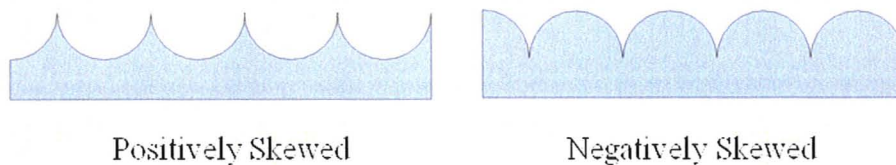


Figure 2.19. Positive and Negatively Skewed Surfaces

During EDM operations the size of each crater depends on the amount of energy expended for each spark. The energy is dependent on the intensity of the spark and the time it flows, both of which affect the metal removal rate and surface finish. Less discharge energy means better surface finish but lower removal rates [37].

Material removal rate and surface texture parameters are determined mainly by the time between two pulses and the pulse width of the spark. The shorter the time between two pulses and the greater the spark discharge power the greater the material removal rate [38]. Higher current is used for roughing operations. Higher current will improve material removal rates, but at cost of surface finish leaving a rougher surface with deeper craters [39].

With longer pulse on time more workpiece metal is melted away. The resulting crater is broader than with a shorter pulse time. Longer pulse time also means more heat and larger recast layer to be considered [39].

Some consideration has to be taken for the effect of the heat generation during EDM on the workpiece structure. After an EDM operation, a top white layer crystallizes from the liquid cooled at high speed. Below the top layer is a chemically affected layer with change in chemical composition and phase changes. The surface is also spattered with expelled molten material that is recast, much like laser machining which may need to be removed prior to testing. Due to the intense heat generation micro cracks can form in the white layer affecting the strength of the machined surface [39].

To control the depth of the craters the gap size between workpiece and electrode must also be considered. Gap size between the electrode and workpiece is on the order of 1 to 50 micro meters, and increases with increase in peak discharge current due to production of more debris in gap. Pulse on time has slight increase on machining gap also due to increase in machining debris. Duty factor and peak discharge current are most important factors that affect gap size, increase in either causes increase in gap size [40].

Dimpled and linear textures have been shown to be effective at reducing friction in multiple applications, under different speed, load, and oil viscosity conditions. Optimum texture configurations were found to be based on the operating conditions, resulting in dimple textures and linear textures specific to operating conditions. The textures have been manufactured by several different processes, such as laser machining, ECM, grinding, etc, which can be time consuming and expensive. EDM can produce similar textures rapidly. An isotropic surface can be easily manufactured, and the characteristics of the texture quickly modified by changing the EDM process parameters. A significant reduction in friction will be demonstrated using EDM textured cutting tools in Chapter 4.

## **Chapter 3**

### **Experimental Details**

This thesis is experimental in nature. The objectives of this work were too:

1. Prove the concept of texturing cutting tools using EDM
2. Characterize the associated force reduction
3. and examine aspects of texturing and cutting parameters towards maximizing force reduction

The techniques and equipment that were used in texturing cutting inserts and testing them are outlined in this chapter.

#### **3.1 EDM Setup**

EDM texturing of cutting inserts was performed on an Agietron Impact 2 Sink Ram EDM system (Figure 3.1), using electrical grade copper electrodes.

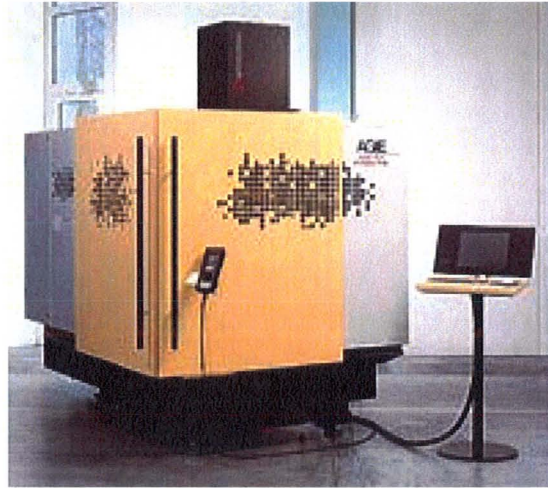


Figure 3.1. Aigetron Impact 2 Ram EDM

The machine tool used EDM Super Supreme dielectric fluid manufactured by Common Wealth Oil.

### **3.2 Textured Cutting Inserts**

As previously reviewed in Chapter 2 the effectiveness of both dimpled and linear textures for improving lubrication was tested.

#### *3.2.1 Cutting Inserts*

Cutting inserts used for experimentation were of SPG 432 geometry and made of T-15 grade high speed steel manufactured by Arthur R Warner Co. This configuration was chosen for the simple geometry, featuring a 0 degree rake angle and 11 degree clearance angle. This allowed for orthogonal cutting, and the unobstructed flat rake face facilitated simple EDM texturing.

### 3.2.2 Dimpled Texturing of Cutting Inserts

The rough dimpled pattern used was manufactured by die sinking an electrode onto the surface of the cutting insert, as seen in Figure 3.2 below. Electrical grade copper electrodes were used in with the face of the electrodes of size 1 cm x ½ cm.

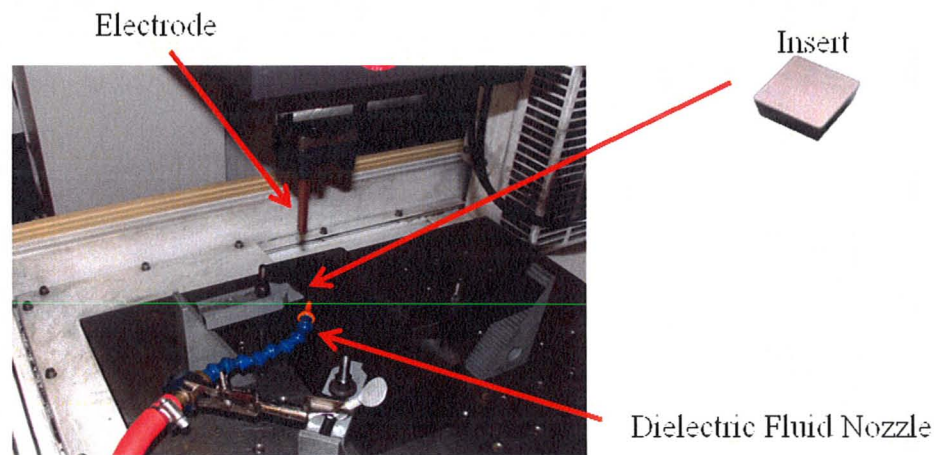


Figure 3.2. Insert Texturing Setup

For a given cutting edge on an insert, only half the face was textured as shown in Figure 3.3 such that textured and non textured surfaces with a similar cutting edge radius could be realized for proper comparison. EDM parameters used will be mentioned in specific sections as appropriate. The inserts were textured such that the grinding direction was perpendicular to the chip flow direction as this has been found to correspond to minimal cutting forces [30][31] [32]. A graphical representation of a cutting insert with textured and non textured edge can be seen in Figure 3.3 below.

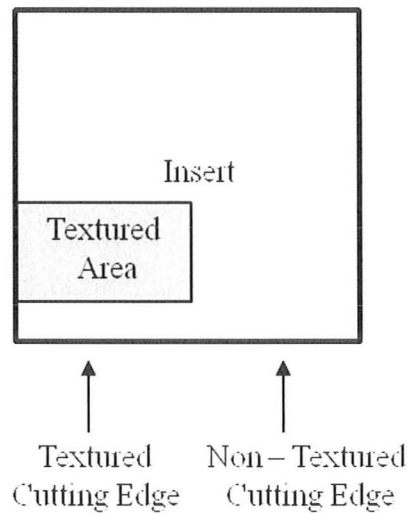


Figure 3.3. Insert Showing Textured Region

### 3.2.3 Linear Textured Inserts

Cutting inserts with linear textures on the rake face were also manufactured and tested. All procedures and the machine tool used were similar to the dimpled textured inserts however the copper electrode used was shim stock of  $75\ \mu\text{m}$  thickness. Each slot was created individually with the electrode moved over a given distance between slots, to create the slotted texture. A representation of the linear texture can be seen in Figure 3.4. Again a comparison between textured and non textured inserts was completed using a single insert.

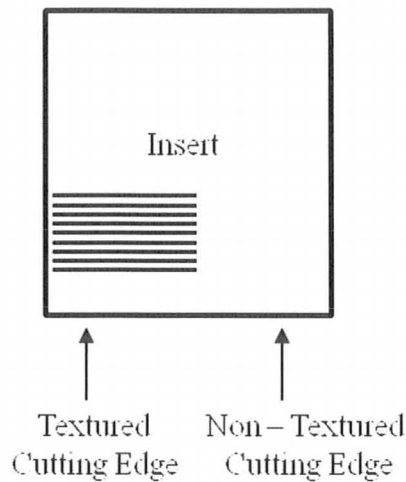


Figure 3.4. Linear Textured Insert with Textured and Non Textured Cutting Edge

### 3.2.4 Texture Characterization

Surface profiles of the dimpled and linear textured inserts were acquired using a Mitutoyo Formtracer CS-5000, with a Cone Stylus F422713/200074 with a tip radius of  $5.0\ \mu\text{m}$  and tip angle of 40 degrees. Profile measurements were taken across the surface of the insert with a spacing of  $0.25\ \text{mm}$  between passes and a measurement pitch of  $5.0\ \mu\text{m}$ . A measuring speed of  $2.0\ \mu\text{m}/\text{sec}$  was used, with 10 passes being recorded for each insert in both directions in order to capture the variability in the surface.

### 3.3 Experimental Test Setup

The purpose of the experimentation was to determine the types of textured cutting tools manufactured that were most effective in reducing the friction and forces, and to identify the machining conditions under which such force reductions were materialized. As such various test conditions were used and will be listed in their respective sections.

All inserts were tested on a Nakamura SC- 450 Lathe with oil lubricant. Cutting Oil 250 A (see Table 3.1 for properties) manufactured by Chem Ecol, which is a light duty cutting oil with synthetic fat additives for improved cutting on metals such as aluminum. The Nakamura SC-300 Lathe test setup is shown in Figure 3.5.

Table 3.1. Properties of Chem Ecol 250 A Cutting Oil

Viscosity @ 40 C	37 cSt
Specific Gravity	0.9

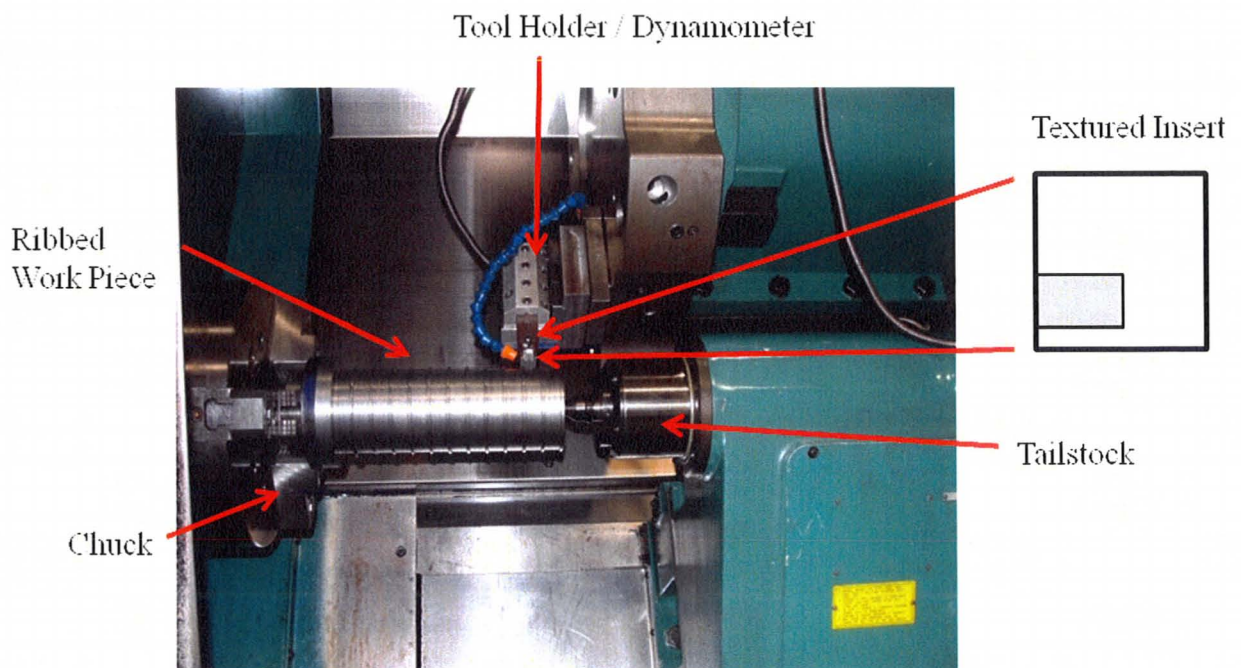


Figure 3.5. Nakamura Tome Sc-459 Lathe Test Setup

A Kistler 3 Force Toolholder Dynamometer Type 9121 was used to measure cutting forces, in conjunction with three Kistler Type 5010 Dual Mode Amplifiers and

Labview program to record cutting forces. Sampling rates of 100 to 500 samples per second were used.

### 3.3.1 Oil Supply

Oil supply for lubricated cutting was from the rear along the rake face of the tool, shown in Figure 3.6 as per research conducted by Childs, De Chiffre, and Shaw [11][14][41], which corresponded to optimal lubricant penetration through micro channels and capillary action.

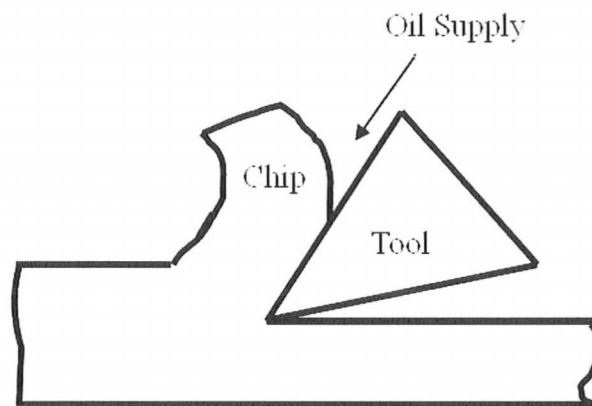


Figure 3.6. Oil Supply Direction

This was confirmed by testing the direction of the lubricant nozzle relative to the tool rake face from above, rear, side and both sides to determine their effectiveness. The test was performed at a 0.1 mm uncut chip thickness and cutting speed of 2 m/min with initial EDM parameters and X distance 0.2 mm to test variations of the nozzle direction.

Table 3.2. Cutting Forces with Various Nozzle Configurations  
Continuous Cutting 1045 Steel  $t = 0.1$  mm  $V_c = 2$  m/min  $X = 0.2$  mm

<i>Nozzle Configuration</i>	<i>Percent Reduction in Feed Force</i>	<i>Percent Reduction in Cutting Force</i>
One Nozzle Above	27	12
One Nozzle Side	27	11
One Nozzle Each Side	27	11
Both Nozzles From Rear	27	11

As can be seen the nozzle configuration has minimal effect on the force reduction, and the process is very similar to flood lubricant. Even a minimal amount of lubrication can affect friction as determined by da Silva [10], and as such rear mounted lubrication will be used as per standard machining practice.

### 3.3.2 Calibration

The Kistler Dynamometer was calibrated with weights and compared to a Microtest Strain Gauge Model CTC/3kN to confirm the accuracy of the calibration data provided by the manufacturer. The Dynamometer was found to be accurate within 1.5% with weights ranging from 11 to 80 kilograms and within 1% of values obtained with the Microtest Strain Gauge. The weights were measured with an Intercomp E-Z WEIGH Scale Model SW500.

A drift analysis was performed on the measurement setup. 10 tests of 10 minute durations were performed with a sampling rate of 200 samples per second with no load. It was found the signal drifted consistently by 1.4% after 10 minutes and the drift was linear

in nature and thus easily compensatable. Most cutting tests conducted were less than 1 minute in duration.

### 3.3.3 Test Samples

Ribbed test samples of 1045 Steel and 6061 Aluminum ranging from 50 to 127 mm in diameter were used. The rib width was 3 mm which was less than the width of the tool (12.5 mm) allowing for orthogonal testing, and spacing between the ribs was 18 mm to allow for sufficient room to position the toolholder between ribs without cutting into adjacent ribs, as shown in Figure 3.7 and Figure 3.8. Sampling rate used for continuous cutting was 200 samples/second.

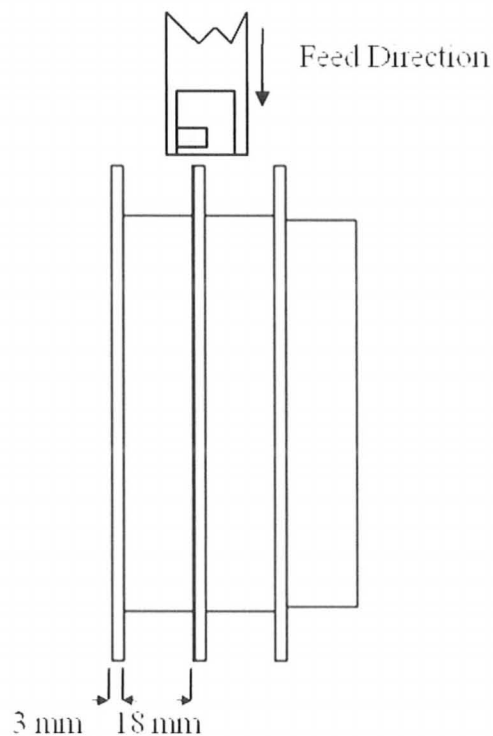


Figure 3.7. Dimensions of Workpiece

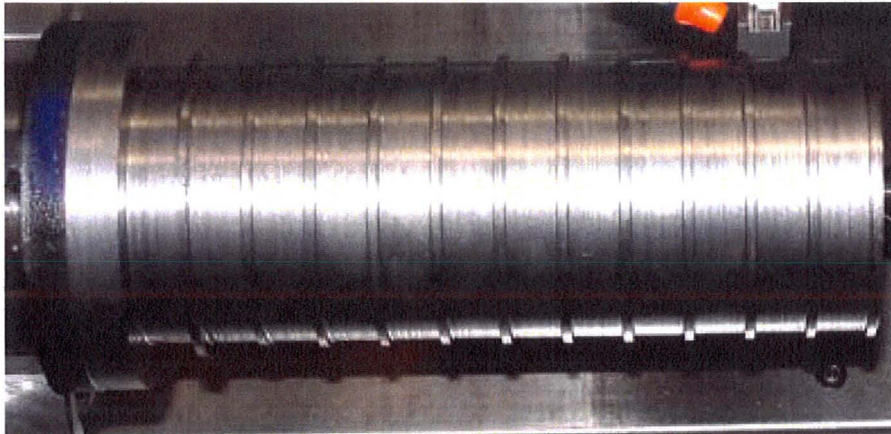


Figure 3.8. Ribbed 1045 Steel Test Sample

#### *3.3.4 Interrupted Cutting*

To test the effect of cutting over finite distances interrupted cuts were also tested. Interrupted cutting on the lathe was accomplished by milling slots along the length of the test samples. Four slots of 12.7 mm wide were milled at 90 degrees apart, as seen in Figure 3.9 . Figure 3.10 shows a photograph of the actual workpiece. By varying the diameter of the workpiece the frequency of interruption changes. This allows for simulation of interrupted cuts such as those in broaching operations to determine if there was a minimum length of material for effectiveness of the inserts and for comparison with continuous cutting, as those experienced in low speed cutting operations such as broaching. The sampling rate for interrupted cutting was 500 samples/second to allow for the small cutting distances

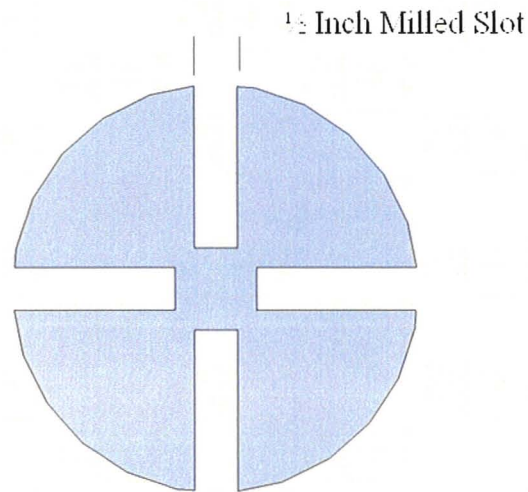


Figure 3.9. Cross Section of Interrupted Test Samples Showing the Slots



Figure 3.10. Interrupted Cutting Test Sample

### 3.4 Test Procedure

#### 3.4.1 Preliminary Testing

Childs [9] indicated that the effectiveness of cutting lubricants maximized at low speed cutting. As such initial testing was conducted at a low cutting speed of 2 m/min, with uncut chip thickness ranging from 0.025 mm to 0.1mm.

All inserts were textured on the EDM with a gain of 15, compression of 20, and voltage of 160 V. EDM parameters were modified to vary the surface created. Discharge and Pause Time modified the width of the craters formed. The current modified the depth of dimples created. The polarity changed the dominant wear pattern from insert to electrode. Cutting parameters initially tested were as seen below;

Table 3.3. Cutting Parameters of Initially Tested Insert

<i>Discharge Time(<math>\mu</math>s)</i>	<i>Pause Time(<math>\mu</math>s)</i>	<i>Current (Amps)</i>	<i>Polarity</i>
42	42	39	+

A polished insert with a roughness Ra  $6.3 \times 10^{-7} \mu\text{m}$  was also used for comparison.

The change in cutting forces experienced was computed using the following formula:

$$\text{Percent Reduction in Force} = \frac{\text{Force of Textured Inserts} - \text{Force of Non Textured Inserts}}{\text{Force of Non Textured Inserts}} \quad (3.1)$$

The force of the textured and non textured insert refers to the either the cutting or feed force of the respective insert.

### 3.4.2 Non-Textured Edge Testing

The effect of the distance between the cutting edge and the location of the texture, as seen in Figure 3.11 was also experimentally tested. Initial EDM test parameters were used to determine the optimum distance X required for maximum force reduction. The distance X was measured on the Mitutoyo Formtracer CS-5000.

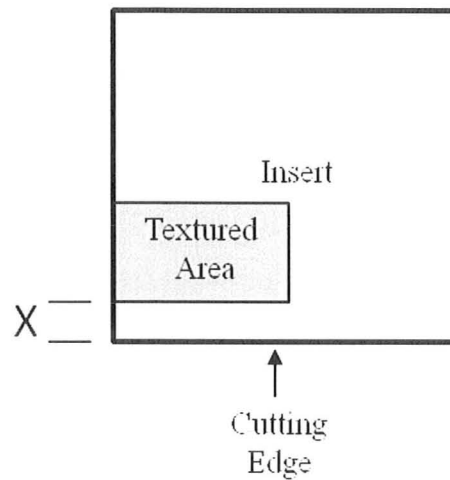


Figure 3.11. Definition of Non Textured Gap Size X

The distance X varied (from 0 to 0.4 mm), giving a varying space between cutting edge and texture, a representation of which can be seen in Figure 3.12 below.

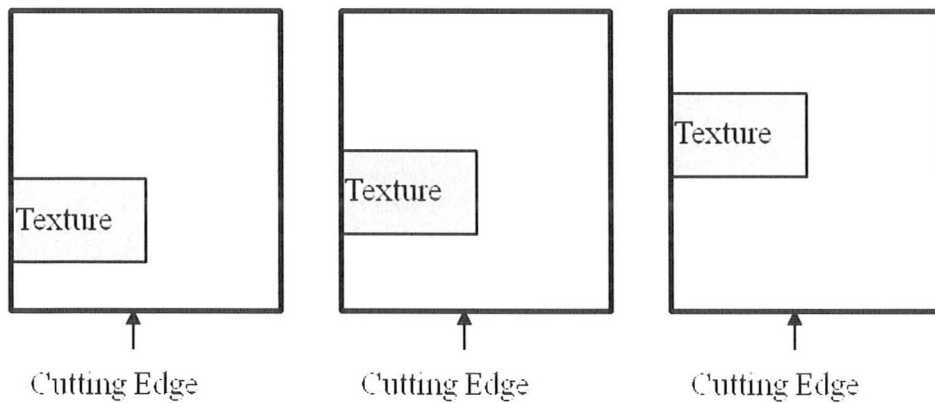


Figure 3.12. Progression of Non Textured Gap Size

The samples were tested on 1045 steel, with an uncut chip thickness of 0.025, 0.05, and 0.1 mm, at a cutting speed of 2 m/min.

### *3.4.3 Tool Chip Contact Length*

The tool chip contact length at the interface between the tool and chip was experimentally determined using Dykem Blue applied to the rake face of the cutting inserts. The face of the inserts was cleaned prior to application of the Dykem Blue with alcohol swabs. When the chip passes over the face of the tool the blue is worn away allowing for easy visual measurement of the maximum contact length.

### *3.4.4 EDM Parameter Comparison*

The Discharge Time and Current was varied based around the previously mentioned preliminary starting parameters to determine if different EDM parameters may prove more beneficial by influencing depth and diameter of the formed dimpled textures, as has been noted in previous experiments with lasers [23] [24][25] [26][27]. The following EDM Parameters were used, with a previously determined effective non textured gap size. By increasing the on time  $T$ , textures with wider dimple features were created. Increasing current  $I$  leads to dimple features with increased depth. Modification of these parameters determined if there was an optimal EDM setting, and thus surface features formed. The uncut chip thickness and cutting speed used were 0.1 mm and 2 m/min respectively, with a distance  $X$  optimized for the uncut chip thickness, which will be mentioned further.

Table 3.4. EDM Parameter Testing

$T(\mu s)$	$I(Amps)$
42	10
42	21
42	52
42	72
42	39
10	39
24	39
87	39
133	39

### 3.4.5 Linear Textures

Work conducted by Sugihara [33] and Berlet [34] indicated the possibility of using linear textures on cutting inserts to reduce friction. These inserts were tested by using slots of increasing area density to determine an optimum textured surface area for force reduction. The following inserts were used with different slot densities as seen in Table 3.5. The EDM parameters used were those of the initial testing.

Table 3.5. Linear Texture Configuration

$X(mm)$	<i>Slot Width (mm)</i>	<i>Texture Spacing (mm)</i>	<i>% Surface Removed</i>
0.2	0.1	One Line	N/A
0.2	0.1	0.35	22%
0.2	0.1	0.3	25%
0.2	0.1	0.08	53%
0.2	N/A	Solid	100%

### *3.4.6 Cutting Parameters*

The cutting parameters, namely cutting speed and uncut chip thickness, were varied to determine the range in which lubrication could be effective, as per the work of Childs [9] who noted the effectiveness of lubricants decreased with increasing cutting speed. He also noted based on uncut chip thickness and cutting speed there was a range of the two parameters where in lubrication could be effective. The affect of the textured inserts on the operating range was determined.

## **3.5 Surface Roughness**

Aside from a reduction in friction, the textured surfaces might also maintain or reduce the surface roughness of the workpieces. Machined surfaces were compared at different uncut chip thicknesses to study the difference in resulting surface roughness.

All results referring to the use of EDM textured insert can be seen in Chapter 4. A significant force reduction using textured inserts is demonstrated, as well as the cutting parameters pertaining to such reductions. Appropriate tool geometry required is determined and resulting surface finish data is presented.

## Chapter 4

### Results and Discussion

The application of using EDM to texture cutting tools is a novel one. To the best of the author's knowledge there is no previous work reported on this innovative approach that expands the application of EDM in tool manufacture. The different components of the experimental work conducted are depicted below:

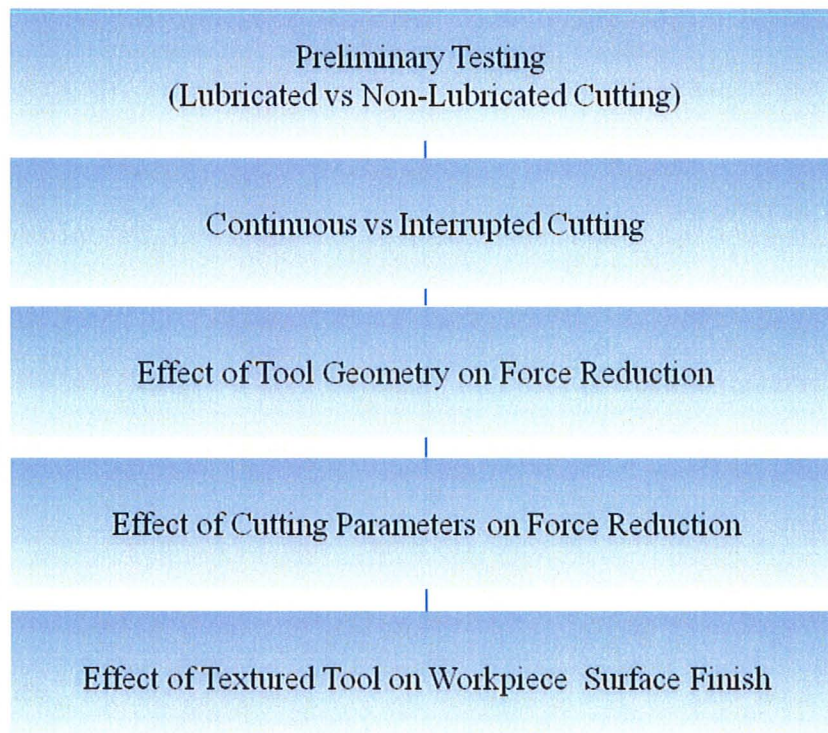


Figure 4.1. Flow Chart Outlining Experimental Work Presented in Chapter 4

#### 4.1 Force Relation Between Measured Forces and Tool Forces

The geometry of the inserts used and the tool holder were chosen such that cutting test pertained to an orthogonal (2 dimensional) configuration. The  $F_x$  and  $F_z$  forces measured with the dynamometer referred to the Feed ( $F_q$ ) and Cutting Force ( $F_p$ ) respectively.

Representing the cutting forces in the form of a Merchant's Circle (Figure 4.2), the relation between the feed and cutting forces to the force tangential ( $F_c$ ) to the rake face of the cutting tool can be determined as:

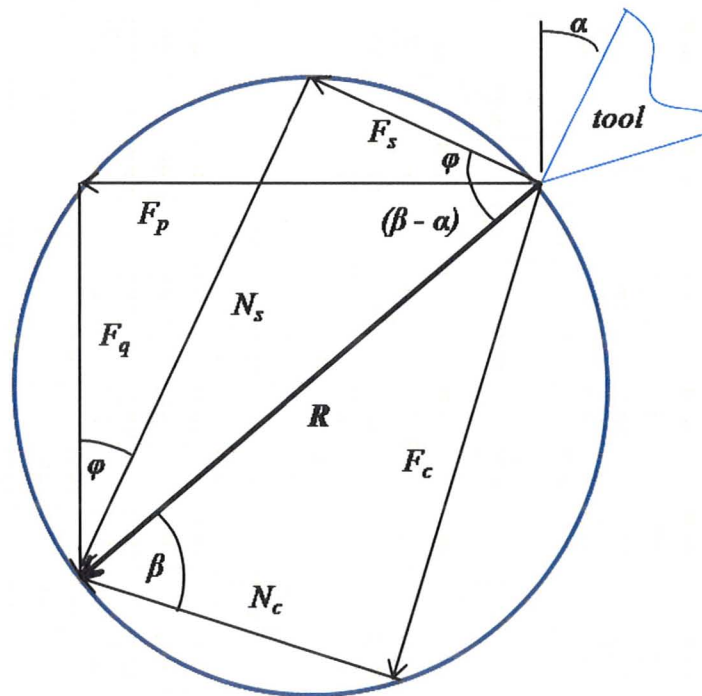


Figure 4.2. Merchant's Circle Diagram

$$F_c = F_p \sin \alpha + F_q \cos \alpha \quad (4.1)$$

where  $\alpha$  is the rake angle. With a zero degree rake angle as used in this work, the friction force ( $F_c$ ) works out to be the same as the feed force ( $F_q$ ), as shown below.

$$F_c = F_q \quad (4.2)$$

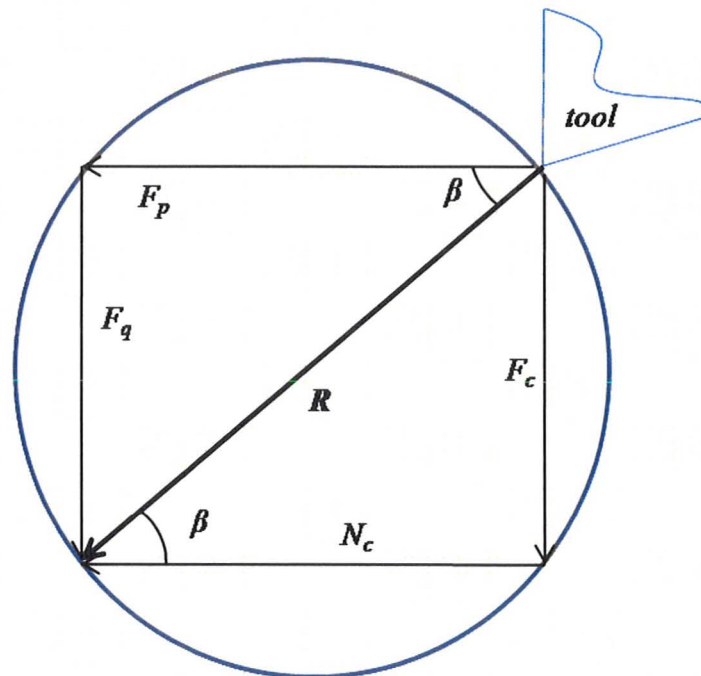


Figure 4.3. Merchant's Circle Diagram with  $\alpha = 0^\circ$

## 4.2 Force Time Plots for Lubricated and Non Lubricated Cutting

Figure 4.4 and Figure 4.5 show the time evolution of feed and cutting forces respectively, to compare the performance of texture and non-textured inserts, under lubricated and non-lubricated conditions. Lubrication was applied at the beginning of the test, and then turned on and off intermittently during the course of cutting. Cutting was conducted at a speed of 2 m/min and an uncut chip thickness of 0.1mm, with a tool optimized for this uncut chip thickness using initial EDM parameters ( $T = 42 \mu\text{s}$ ,  $P = 42 \mu\text{s}$ ,  $I = 39 \text{ Amps}$ ,  $V = 160 \text{ V}$ ) and a X distance of 0.2 mm. Oil penetration was from the

rear of the tool as per research conducted by Childs, Shaw, etc [11][14][41], for better lubricant penetration.

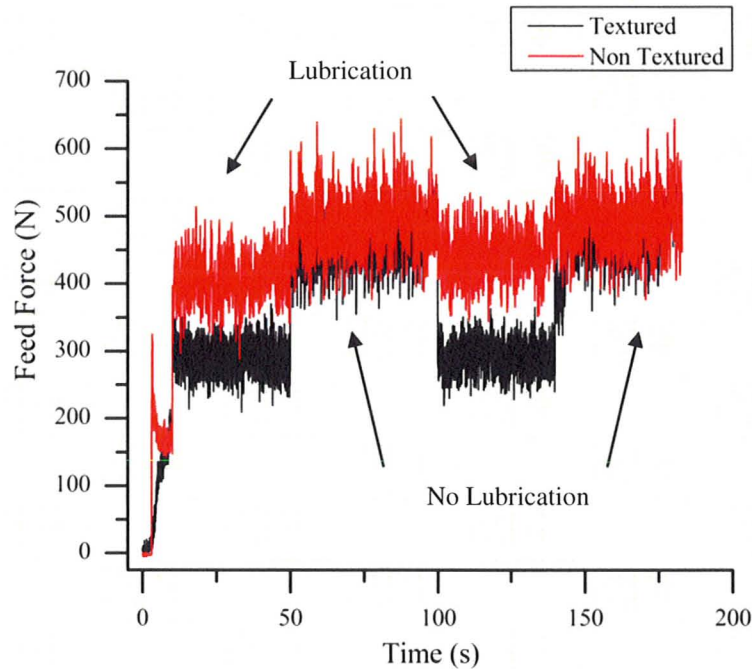


Figure 4.4. Comparison of Feed Force between Non Textured and Textured Inserts – Continuous Cutting 1045 Steel  $t = 0.1$  mm  $V_c = 2$  m/min  $X = 0.2$  mm

The data in Figure 4.4 and Figure 4.5 are very conclusive in showing the effectiveness of the EDM texturing process in terms of force reduction. It is clear that the drop in forces is rather instantaneous with the application of the lubricant, and that the reduction in the feed force is more marked as compared to the reduction in the cutting force.

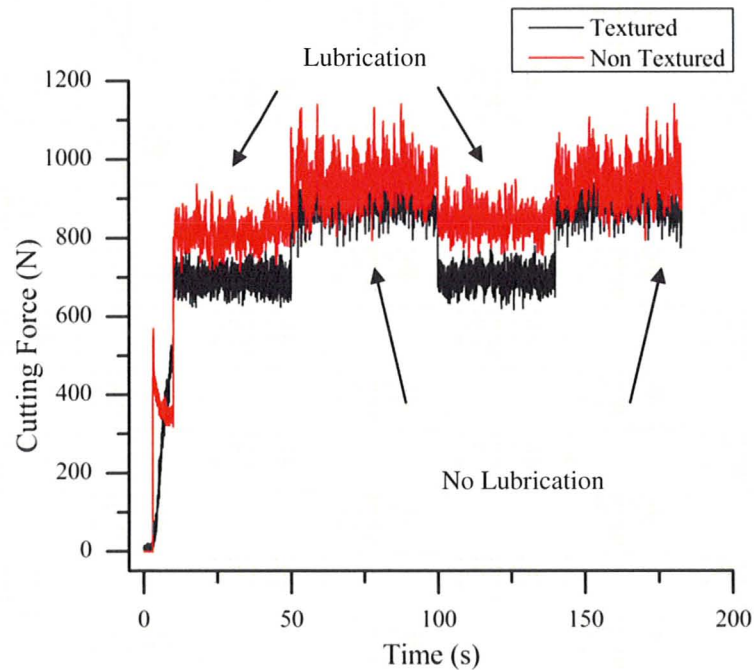


Figure 4.5. Comparison of Cutting Force between Non Textured and Textured Inserts – Continuous Cutting 1045 Steel  $t = 0.1$  mm  $V_c = 2$ m/min  $X = 0.2$  mm

There is a reduction of the machining forces when lubrication is applied for both the textured and non textured inserts however the textured insert corresponded to significantly less force. The texture helps promote the penetration and retention of lubricant at the chip-tool interface. It is also evident that there is a slight reduction in forces when using a textured tool with no lubricant. This is likely due to the texture acting to some extent as a restricted rake face tool owing to material removed off the rake face of the tool, limiting the contact area between the chip and tool.

It was discussed by Kawasegi [32] that textured inserts used in high speed cutting reduced forces by reducing the contact length, and lubrication was not required. He found the effectiveness of textures in reducing cutting forces occurred only at high speeds with

or without external cutting fluids. This is thought to be in part due to the tool acting as a restricted rake face tool, and as the workpiece softening and acting as a lubricant, as it has been demonstrated that lubrication is required for significant force reduction.

It is to be noted that that just the sufficient material needs to be removed from the rake face of the tool but for which it acts as a restricted contact tool that could correspond to higher tool stresses despite a reduction in cutting forces.

### **4.3 Effect of Textures on Continuous and Interrupted Cutting**

The effect of the texture in reducing forces was seen for both continuous and interrupted cutting. All cases use lubrication for the entire test as the negative result of dry cutting has been demonstrated and such will not be discussed any further.

#### *4.3.1 Continuous Cutting*

A textured cutting insert was compared to a non textured insert and polished insert at an uncut chip thickness of 0.1mm and cutting speed of 2 m/min for continuous cutting, with an insert textured using initial EDM parameters ( $T = 42 \mu\text{s}$ ,  $P = 42 \mu\text{s}$ ,  $I = 39 \text{ Amps}$ ,  $V = 160 \text{ V}$ ) and X distance 0.2 mm.

A comparison of the average cutting forces and standard deviation of the forces is shown in Figure 4.6, with comparison to a insert with a polished rake face. As can be seen, in addition to a reduction in forces the standard deviation of the forces for the textured inserts is somewhat less than that of the non textured insert. This is due to less adhesion between the tool and chip, reducing the number of welded asperities, reducing

the variation of the signal. A similar effect is reported by Pettersson [30] who noted a reduction in the variation of forces due to less adhesion between surfaces. The average forces of the textured insert were significantly less than that of the non textured and polished inserts.

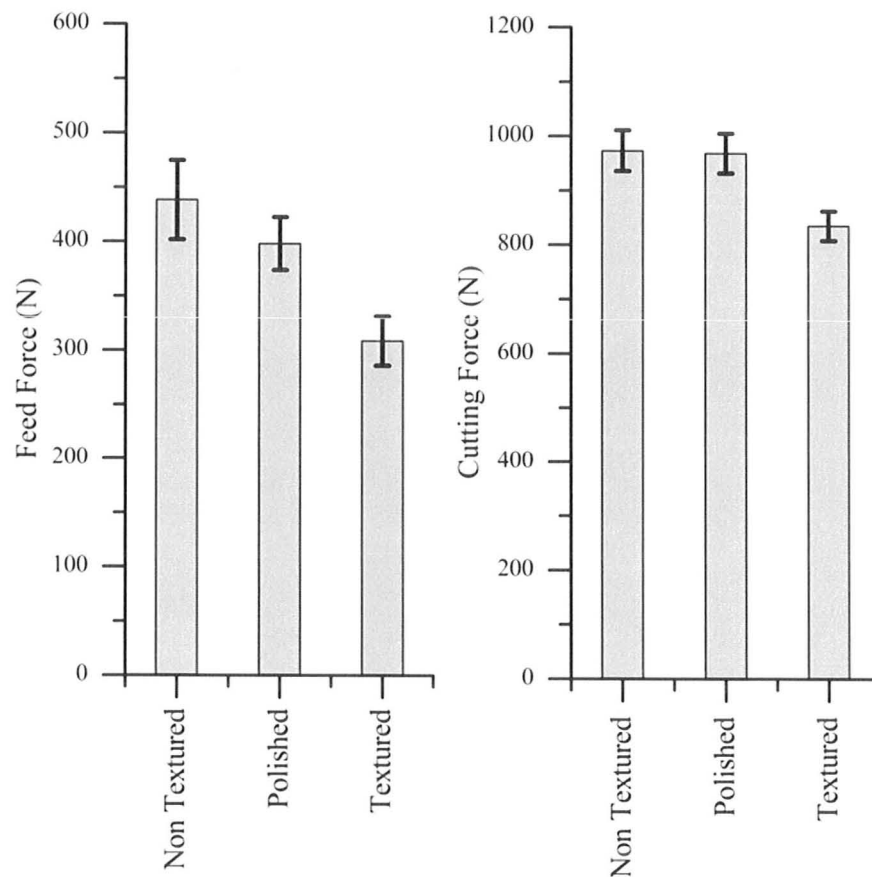


Figure 4.6. Average Feed and Cutting Force Comparison of Inserts - Continuous Cutting 1045 Steel  $t = 0.1$  mm  $V_c = 2$  m/min  $X = 0.2$  mm

#### 4.3.2 Interrupted Cutting

Interrupted cutting was performed to test the effectiveness of the inserts for lubricant retention and penetration when cutting repeatedly over finite cutting distances.

Most of the work on textured tools in the literature has been conducted in continuous cutting operations. As such the effect of cutting with textured inserts in interrupted cutting is not as common. Interrupted cutting was performed at a cutting speed of 2 m/min and uncut chip thickness of 0.1 mm, with a geometrically similar tool as used for the continuous cutting experiment, on a 76 mm diameter workpiece, that resulted in cutting engagement length as seen in Table 4.1.

Table 4.1. Engagement Length of Interrupted Test

<i>Diameter (mm)</i>	<i>Engagement (mm)</i>	<i>Disengagement (mm)</i>
76	46.9	12.7

A comparison between feed and cutting forces relating to textured and non textured inserts can be seen in Figure 4.7 and Figure 4.8, respectively with a significant reduction in forces noted when using a textured insert. The textured inserts also resulted in a decrease in the standard deviation of the forces, as seen in Figure 4.9, similar to the continuous cutting. Polished inserts were not compared as they have been shown (Figure 4.6) to be ineffective in reducing forces significantly and considering this is an operation that adds substantially to the cost of tool manufacture.

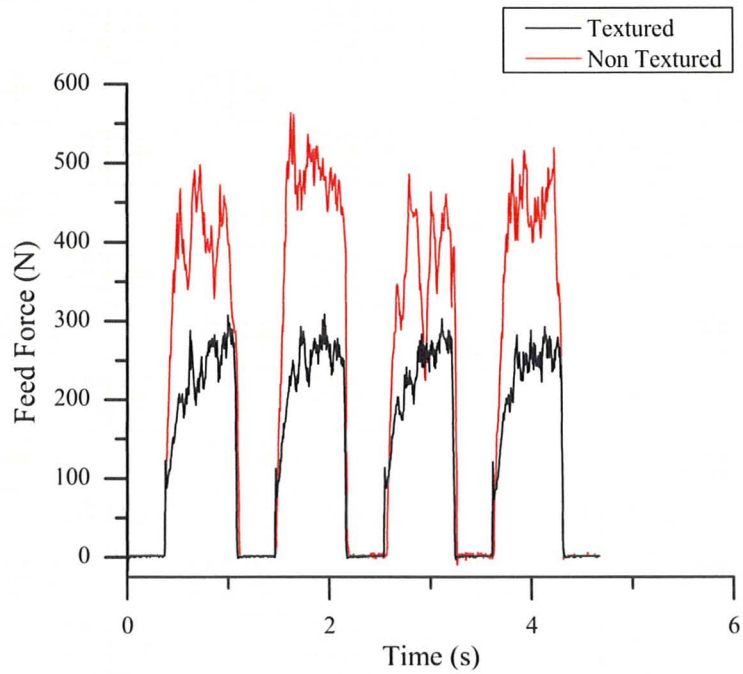


Figure 4.7. Feed Force Comparison between Textured and Non Textured Inserts – Interrupted Cutting 1045 Steel  $t = 0.1$  mm  $V_c = 2$  m/min  $X = 0.2$  mm

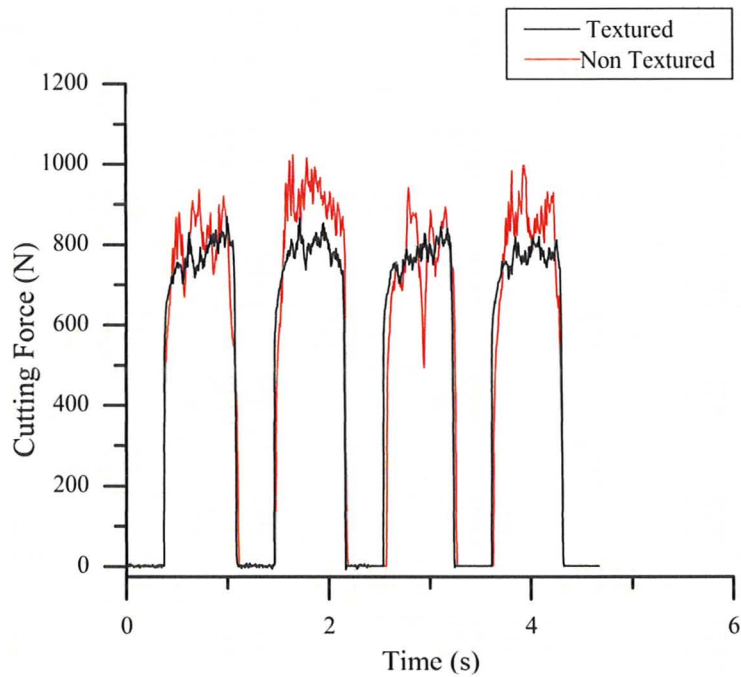


Figure 4.8. Cutting Force Comparison between Textured and Non Textured Inserts – Interrupted Cutting 1045 Steel  $t = 0.1$  mm  $V_c = 2$  m/min  $X = 0.2$  mm

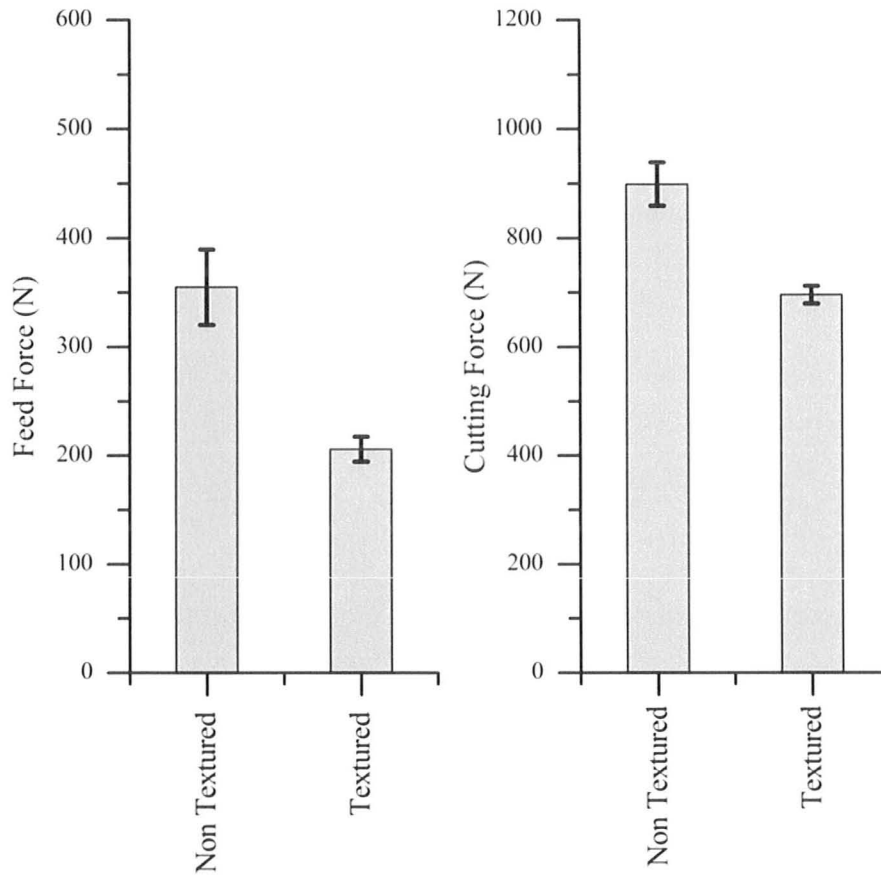


Figure 4.9. Feed and Cutting Force Comparison of Inserts - Interrupted Cutting 1045 Steel  $t = 0.1$  mm  
 $V_c = 2$  m/min  $X = 0.2$  mm

#### 4.4 Components of Force Reduction when using Textured Inserts

A comparison can be seen in Figure 4.10 between continuous cutting with no lubrication, continuous cutting with lubrication, and interrupted cutting with lubrication.

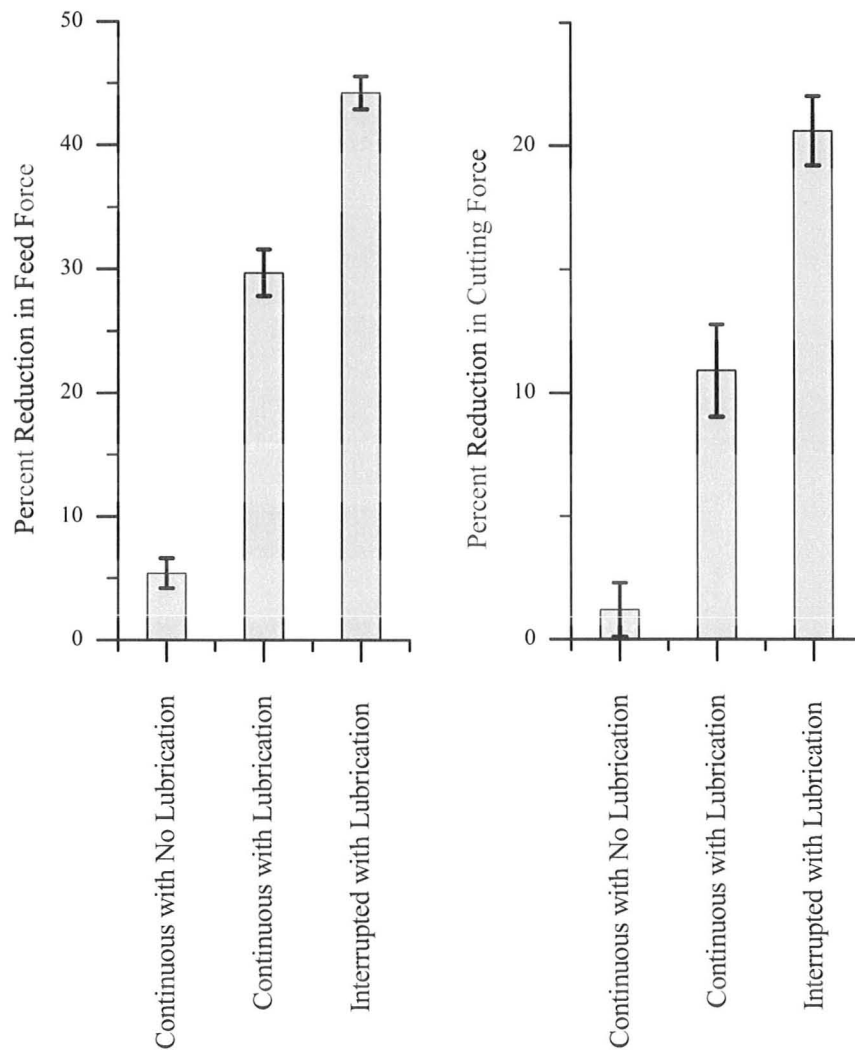


Figure 4.10 Percent Reduction in Feed and Cutting Force Due to Forms of Cutting – Continuous and Interrupted Cutting 1045 Steel  $t = 0.1$  mm  $V_c = 2$  m/min  $X = 0.2$  mm

With continuous cutting and no lubrication a slight reduction in the cutting forces (Figure 4.10) can be seen, due to the tool acting as a restricted rake face tool. When manufacturing the texture, the electrode can be sunk sufficiently past the rake face of the tool such that no contact will occur between the chip and the texture surface when

machining, restricting the size of the rake face.

When continuous cutting with lubrication the force reduction (Figure 4.10) was due to the penetration of the oil and the restriction of the rake face. The reduction of cutting forces when performing interrupted cutting with lubrication (Figure 4.10) was due to enhancing the lubricant penetration but also due to the restriction of the rake face. By removing the effect of the texture in reducing cutting forces with no lubrication, the effect of lubricant penetration and enhanced penetration can be seen in Figure 4.11.

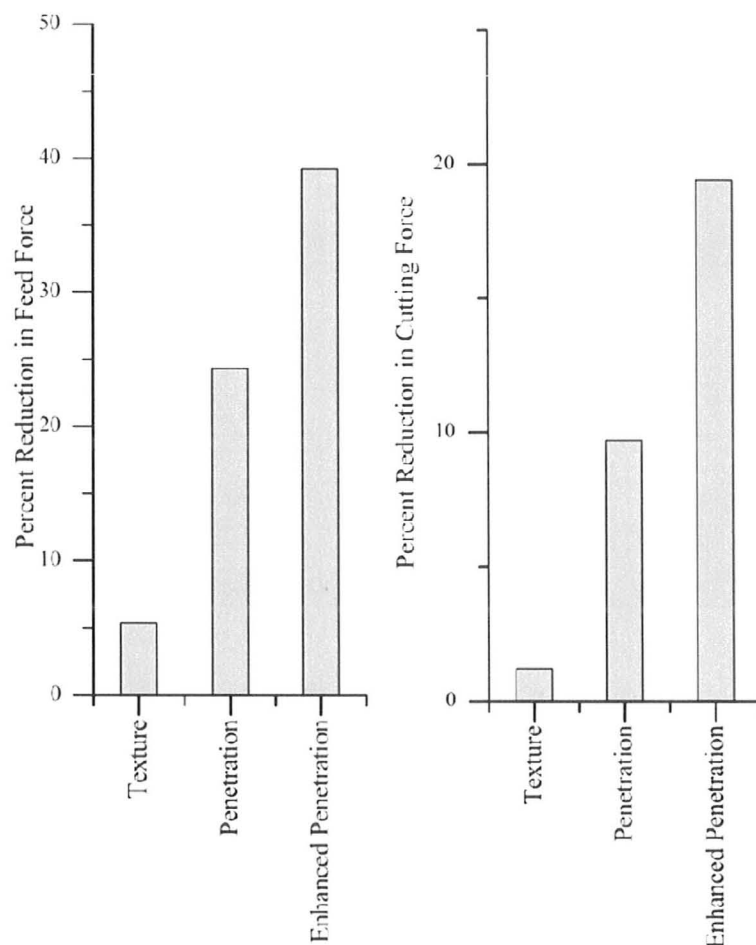


Figure 4.11. Percent Reduction in Feed and Cutting Force Due to Aspects of the Texture - Continuous and Interrupted Cutting 1045 Steel  $t = 0.1$  mm  $V_c = 2$  m/min  $X = 0.2$  mm

Lubricant penetration results in almost a 25% and 10% reduction in feed and cutting force respectively (Figure 4.11). Enhanced penetration and retention of the fluid, due to the increased rake face access from interrupted cutting, accounts for almost a 40% and 20% reduction in feed and cutting forces (Figure 4.11). In an application with finite cutting distances, such as broaching, a significant reduction in cutting forces can be realized compared to continuous cutting.

#### **4.5 Texture Geometry**

The geometry of the texture, in terms of its location with respect to the cutting edge along the direction of chip flow, the percent of the tool surface area textured, and texture surface properties all play an important role in determining the effectiveness of the texture. This is discussed in this section.

##### *4.5.1 Texture Location*

Preliminary testing involved cutting inserts with a non textured edge length of approximately 0.1 mm to retain cutting edge integrity, as per similar work by Jainxin [36] who did not texture all the way to the cutting edge to retain cutting edge integrity. In all cases [32] [33][36] where texturing was used in cutting tools, the spacing of the beginning of the texture was arbitrary or nonexistent, simply to retain tool edge integrity when required. Childs [9] mentioned that in no conditions would lubricant penetrate into the sticking zone, and as such any texture in the sticking zone may hinder the force reduction. Some testing needs to be considered to determine the size of the sticking and sliding zones, which depends on uncut chip thickness. The effect of the non textured edge

length  $X$  (Figure 4.12) is presented in this section. Cutting inserts were used with various non textured edge lengths  $X$  to determine the spacing between the texture and cutting edge that is most effective.

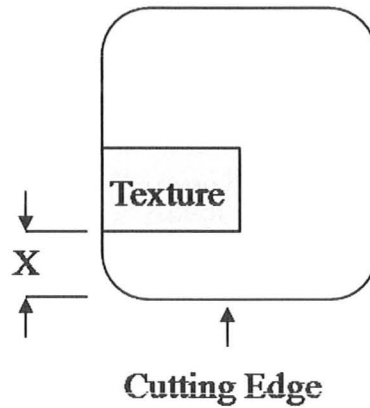


Figure 4.12 Texture Location with Respect to Cutting Edge

The effects of this non textured space as a function of the uncut chip thickness is shown in Figure 4.13.

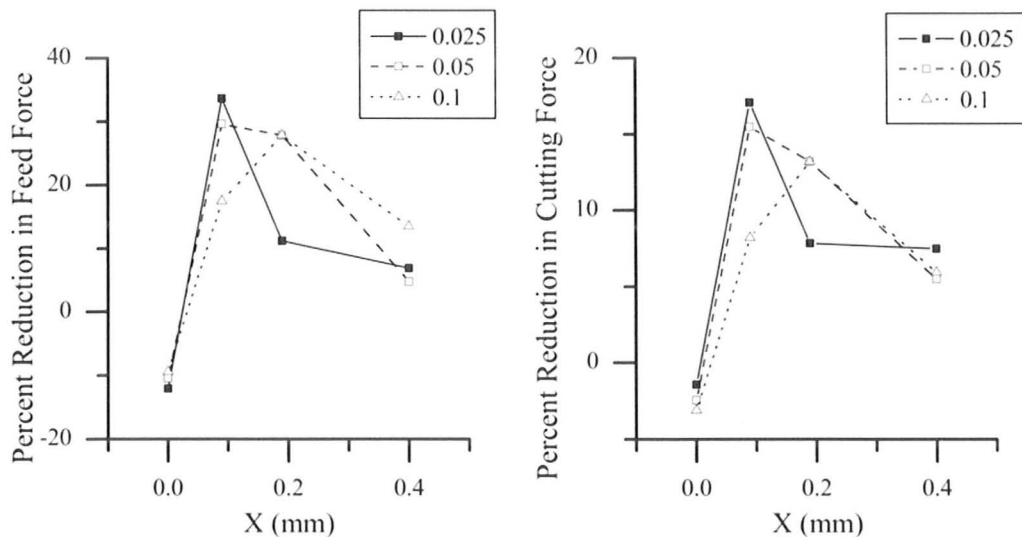


Figure 4.13. Percent Reduction of Feed Force as a Result of Uncut Chip Thickness and Non Textured Edge Length  $X$  - Continuous Cutting 1045 Steel  $V_c = 2\text{m/min}$

With increasing uncut chip thickness the length of the non texture edge length required for maximum force reduction increases. The optimum non textured edge length  $X$  also corresponds to the minimum friction angle resulting in the lowest shearing force required for chip generation. The value of  $X$  was non dimensionalized by dividing by the uncut chip thickness and plotted to show optimum friction angle as seen in Figure 4.14.

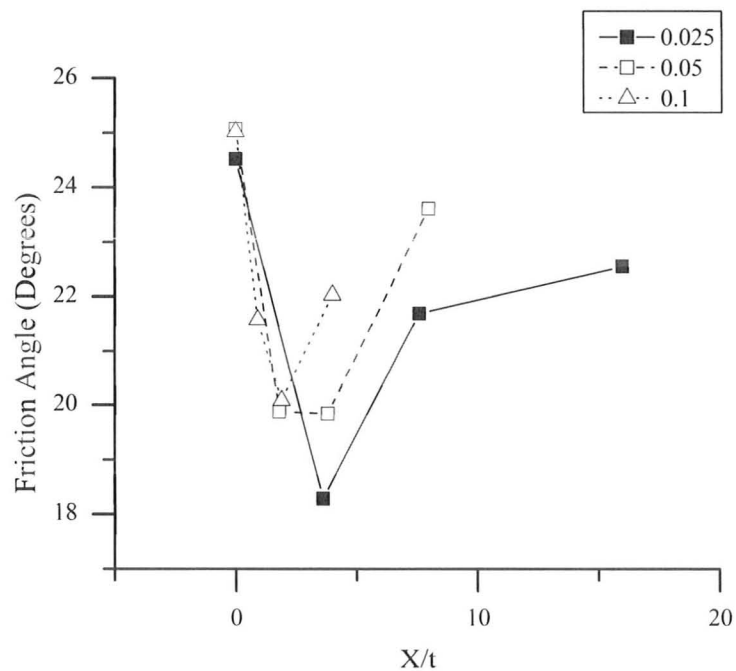


Figure 4.14 Friction Angle as a Result of Uncut Chip Thickness and  $X$  - Continuous Cutting 1045 Steel  
 $V_c = 2$  m/min

As can be clearly seen in Figure 4.13 and Figure 4.14 there is an optimum placement of the texture  $X$  for a particular uncut chip thicknesses. A maximum reduction of cutting forces and friction angle was found for each uncut chip thickness.

At an uncut chip thickness of 0.025 mm a reduction of over 30% in the feed force

and 17% in cutting force was found at an X value of 0.1 mm. At an uncut chip thickness of 0.1 mm a reduction of about 30% in the feed force and 15% in cutting force was found at an X value of 0.2 mm (Figure 4.13).

With increasing distance X past the optimum value the reductions in cutting forces decreased towards those experienced by the non textured tool, as the tool tends to be non-textured

It is interesting to note the texture that extends to the cutting edge slightly increases the forces (Figure 4.13). Cutting force also increased demonstrating that cutting edge integrity is important and should be maintained. The cutting edge radius was measured by the confocal microscope method for the insert that extended the texture to the cutting edge. The edge radius was measured to be 23 micrometers with a standard deviation of 5 micrometers over 20 samples, as compared to 6 micrometers for the non textured tool with a standard deviation of only 0.8 over 20 samples. This indicated that the increase of the cutting edge radius negatively affected the performance of the tool.

As can be seen the optimum placement of the texture (X) is dependent on the uncut chip thickness. With increasing uncut chip thickness, as there is an increasing sticking zone, an increasing non textured gap size is required to maximize the force reduction.

#### *4.5.2 Contact Length Test*

A tool-chip contact length test was performed to determine relation between the

placement of the texture (X) and the size of the sticking zone. Dykem Blue was coated on the insert to determine the contact length.

Consideration was also given to the textures creating restricted rake face tools, by reducing the height of the tool rake surface. This test confirmed that the chip-tool contact length extended into the textured surface, as shown in Figure 4.15, and that the tool was hence not acting as a restricted rake tool.

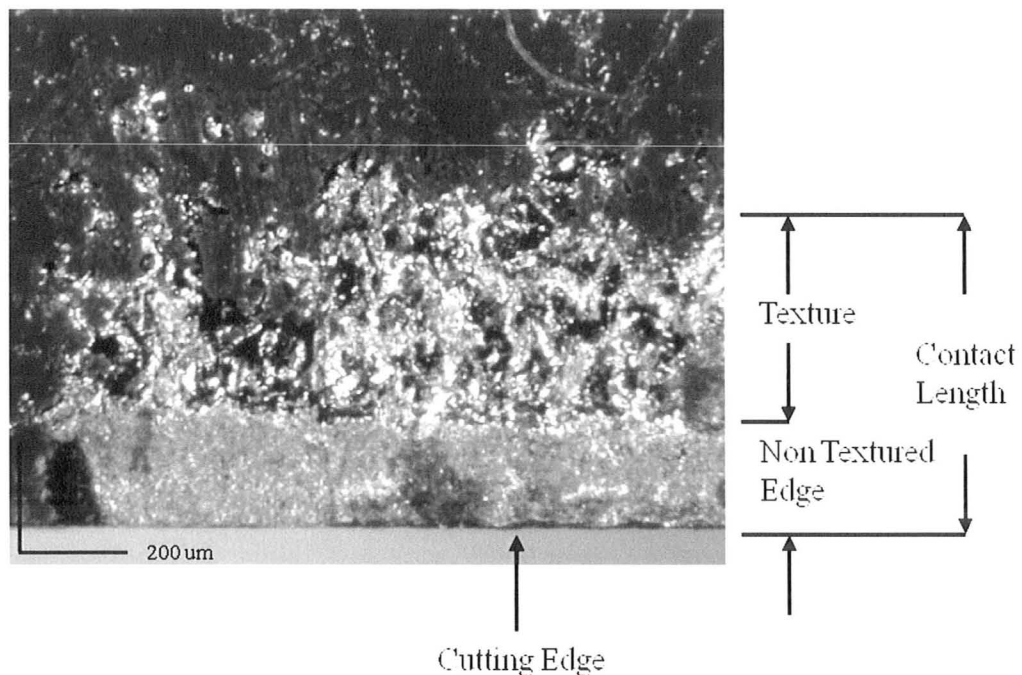


Figure 4.15 Result of Impingement of Chip on Rake Face of Textured Insert - Continuous Cutting 1045  
Steel  $t = 1 \text{ mm}$   $V_c = 2 \text{ m/min}$   $X = 0.2 \text{ mm}$

The tool-chip contact length test was conducted at an uncut chip thickness of 0.025 and 0.1 mm. The results are shown in Table 4.2 and Table 4.3.

Table 4.2. Chip Contact Length Comparison at Uncut Chip Thickness of 0.025 mm - Continuous Cutting 1045 Steel  $V_c = 2$  m/min  $X = 0.09$  mm

<i>Insert</i>	<i>Contact Length (mm)</i>
Non - Textured	0.45
Textured	0.239

Table 4.3. Chip Contact Length Comparison at Uncut Chip Thickness of 0.1 mm - Continuous Cutting 1045 Steel  $V_c = 2$  m/min  $X = 0.2$  mm

<i>Insert</i>	<i>Contact Length (mm)</i>
Non - Textured	0.99
Textured	0.636

A reduction of contact length between textured and non textured samples was seen (Table 4.2 and Table 4.3) as expected, and previously reported by da Silva [10] who noted the effect of reduced contact length with enhanced lubrication.

Assuming 50% of the contact length is sliding and 50% is sticking, the sticking zone incorporates a length of approximately 0.10 mm when testing at an uncut chip thickness of 0.025 (Table 4.2), making the non textured edge length  $X$  and sticking zone approximately the same size.

The same trend is seen when testing at an uncut chip thickness of 0.1 mm (Table 4.3), where the non textured edge length  $X$  is approximately 33% of the sticking zone when lubrication was applied slightly less than expected but still reasonable. The reduction of friction is not as significant comparing an uncut chip thickness of 0.025 mm (Figure 4.13). A greater reduction of friction should be expected when using an insert with a non textured edge length  $X$  closer to 50% of the contact length.

#### 4.5.3 Linear Textures

Cutting Inserts with linear textures were also machined and tested as per research conducted by Kawasegi [32], who investigated the effectiveness of linear textures in cutting applications using laser texturing. The effect of linear texturing the inserts using EDM in reducing forces can be seen in Figure 4.17 and Figure 4.18. By decreasing the spacing between slots (Figure 4.16), the percentage of the surface that was textured was increased. This resulted in the reduction of forces, with the maximum attained when the whole surface was textured.

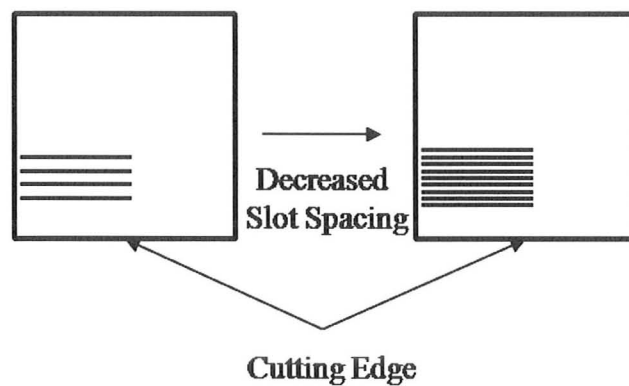


Figure 4.16 Increased Percent of Surface Textured

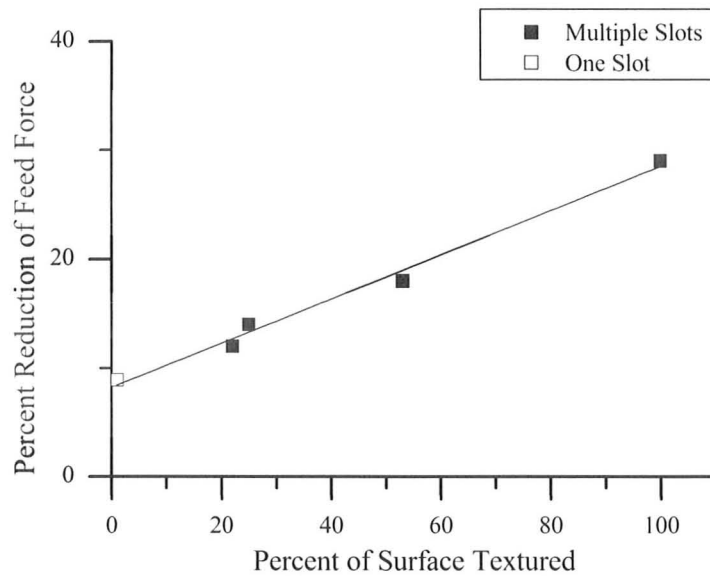


Figure 4.17. Reduction in Feed Force as a Function of Surface Area Textured - Continuous Cutting 1045 Steel  $t = 0.1$  mm  $V_c = 2$  m/min  $X = 0.2$  mm

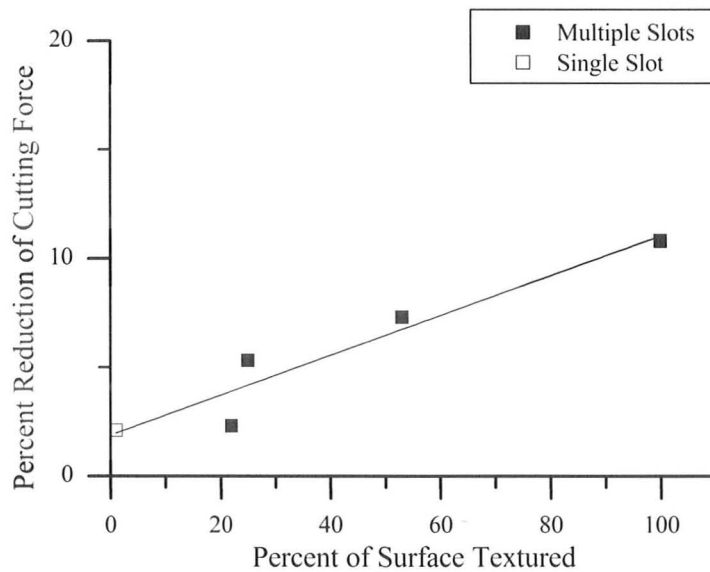


Figure 4.18. Reduction in Cutting Force as a Function of Surface Area Textured- Continuous Cutting 1045 Steel  $t = 0.1$  mm  $V_c = 2$  m/min  $X = 0.2$  mm

As can be seen (Figure 4.17 and Figure 4.18), the greater the area of the insert

textured the greater the reduction in forces, and a completely textured surface is more effective in reducing forces than a slotted textured surface (Figure 4.19).

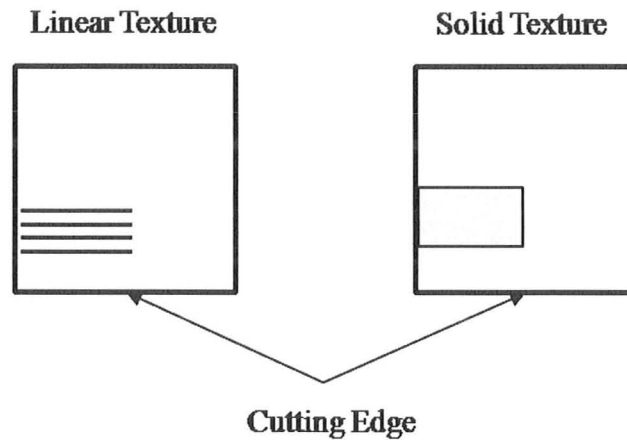


Figure 4.19 Comparison Between Linear Texture and Solid Texture

During the course of running the tests one of the inserts fractured, as seen in Figure 4.20. EDM process results in cracks and thermal stresses in the material being machined. The fracture that occurred could primarily be a result of the EDM process. It is hence recommended that the texture may be introduced during the compaction process and not with a secondary operation like EDM or laser texturing. It should also be noted that only one insert fractured in this form during the course of completion of this research.

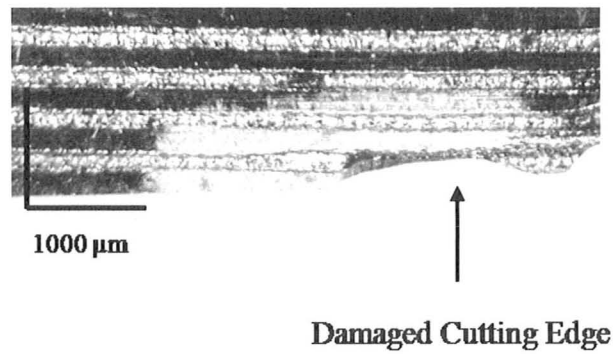


Figure 4.20. Insert Damaged During Cutting

#### 4.5.4 Effect of EDM Parameters

The EDM parameters, specifically the pulse on-time and current, were varied to test their effect when continuous testing with lubrication to determine an optimum roughness. The pulse on-time largely varies the aspect ratio of the formed crater, by increasing the diameter of crater formed, whereas the current increases the depth of crater formed. The uncut chip thickness and speed used were 0.1 mm and 2 m/min respectively, with an X length of 0.2 mm. The effect of varying current and pulse on time can be seen in Figure 4.21 and Figure 4.22, with an optimum current and pulse on-time combination being determined.

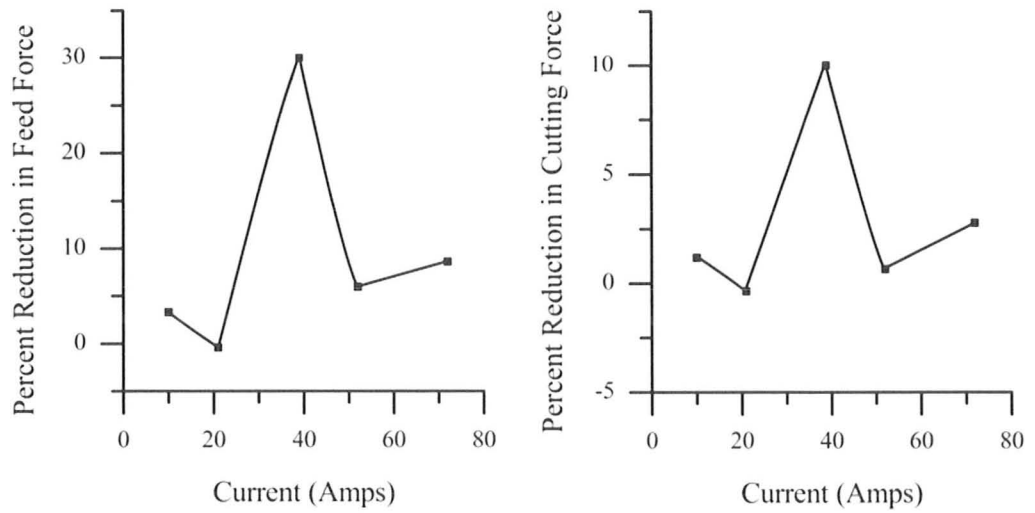


Figure 4.21. Percent Reduction in Force as a Result of Current – Pulse on Time at  $42 \mu\text{s}$  Continuous Cutting 1045 Steel  $t = 0.1 \text{ mm}$   $V_c = 2 \text{ m/min}$   $X = 0.2 \text{ mm}$

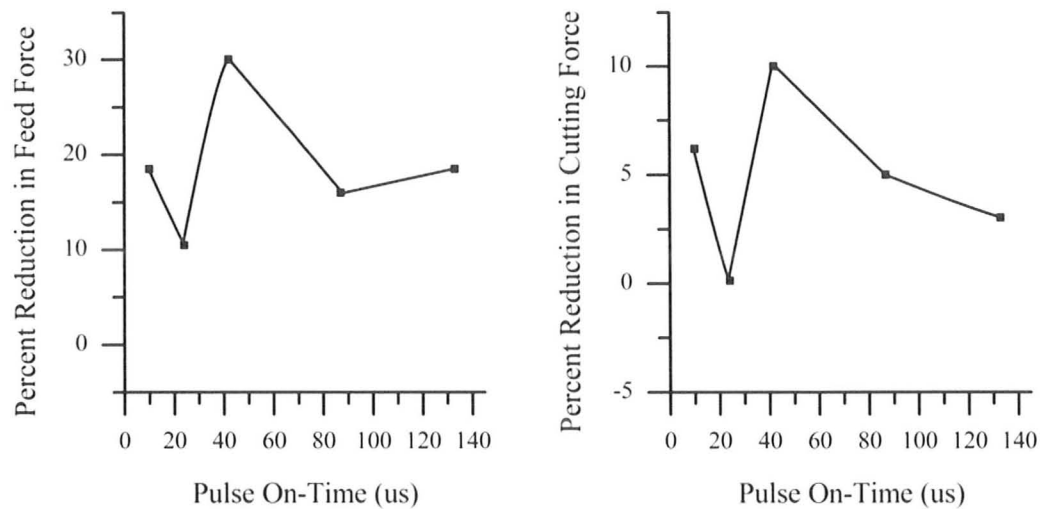


Figure 4.22. Percent Reduction in Force as a Result of Pulse On – Time – Current at 39 amps Continuous Cutting 1045 Steel  $t = 0.1 \text{ mm}$   $V_c = 2 \text{ m/min}$   $X = 0.2 \text{ mm}$

The surface of the EDM texture was characterized to determine what parameters can be used to optimize the texture. The roughness  $R_a$ , skewness and kurtosis of the

EDM surfaces was calculated using the following formulas, where  $n$  represents the number of samples and  $y_i$  is the vertical distance from the mean line to the point;

$$\text{Roughness Ra} \quad Ra = \frac{1}{n} \sum_{i=1}^n |y_i| \quad (4.3)$$

$$\text{Root Mean Squared} \quad Rq = \sqrt{\frac{1}{n} \sum_{i=1}^n y_i^2} \quad (4.4)$$

$$\text{Skewness} \quad Rsk = \frac{1}{nRq^3} \sum_{i=1}^n y_i^3 \quad (4.5)$$

$$\text{Kurtosis} \quad Rku = \frac{1}{nRq^4} \sum_{i=1}^n y_i^4 \quad (4.6)$$

The values of Ra, skewness, and kurtosis calculated in this work (Table 4.4) are similar in magnitude to those found by Londardo [57] for EDM surfaces.

Table 4.4 Surface Characteristics of EDM Texture as a Function of EDM Parameters

<i>Current (amps)</i>	<i>Pulse on Time (us)</i>	<i>Ra</i>	<i>Ra Standard Deviation</i>	<i>Skewness</i>	<i>Skewness Standard Deviation</i>	<i>Kurtosis</i>	<i>Kurtosis Standard Deviation</i>
10	42	6.6	0.523	0.002	0.013	2.234	0.160
21	42	6	1.114	0.493	0.013	3.646	0.099
52	42	11.7	1.169	0.355	0.024	2.971	0.088
72	42	19.65	0.921	0.200	0.019	3.332	0.124
39	42	10.4	1.284	0.102	0.020	2.568	0.071
39	10	4.2	0.827	-0.012	0.016	1.838	0.082
39	24	4.245	1.431	0.445	0.031	3.433	0.178
39	87	5.95	1.323	0.079	0.010	2.358	0.192
39	133	8.6	1.266	0.073	0.016	2.356	0.110

The result of the surface parameters can be seen plotted in Figure 4.23, Figure 4.24, and Figure 4.25.

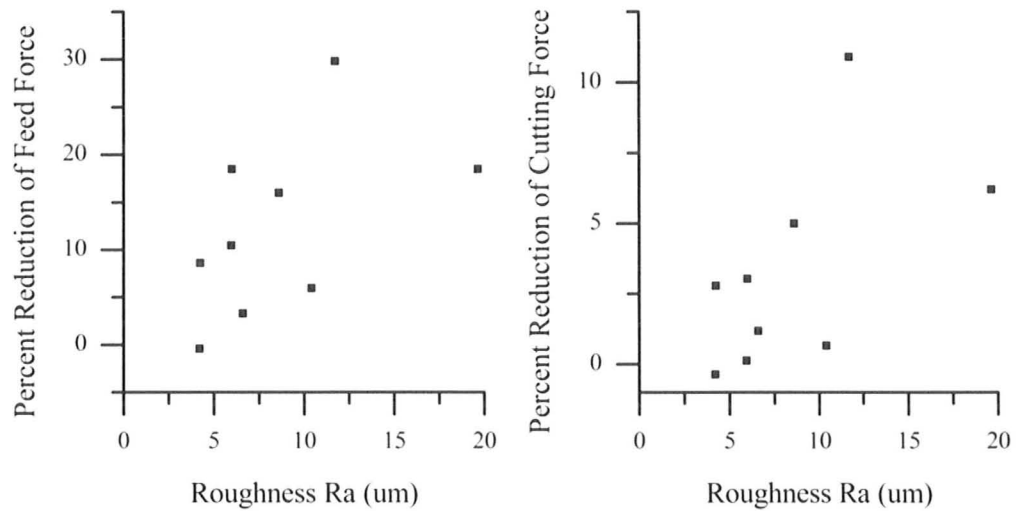


Figure 4.23. Percent Reduction of Feed Force as a Result of EDM Surface Roughness Ra - Continuous Cutting 1045 Steel  $t = 0.1$  mm  $V_c = 2$  m/min  $X = 0.2$  mm

As can be seen in Figure 4.23, there appears to be no direct correlation between the EDM surface roughness and reduction of forces. This is likely due to multiple surface configurations corresponding to similar Ra values. More information is hence required to define a surface, such as skewness and kurtosis.

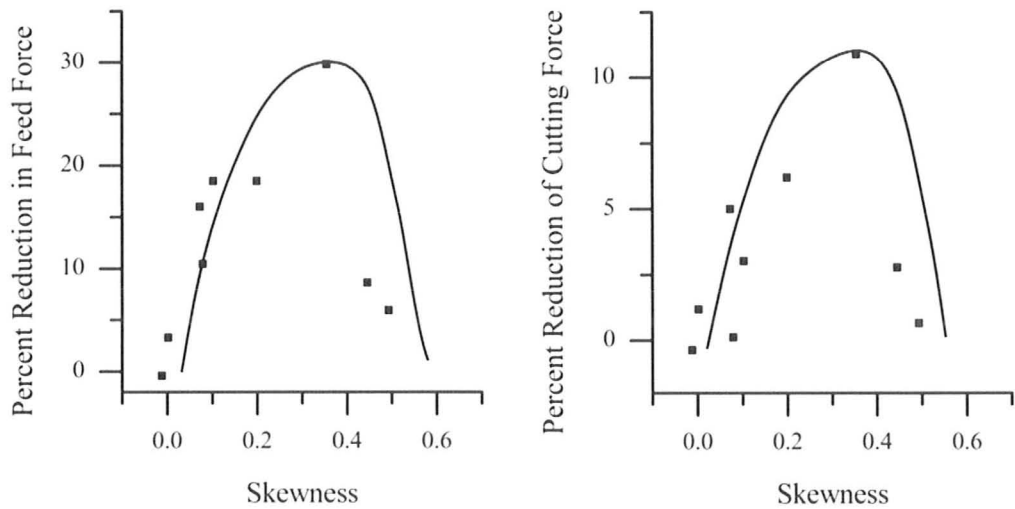


Figure 4.24. Percent Reduction of Feed Force as a Result of EDM Surface Skewness - Continuous Cutting  
1045 Steel  $t = 0.1$  mm  $V_c = 2$  m/min  $X = 0.2$  mm

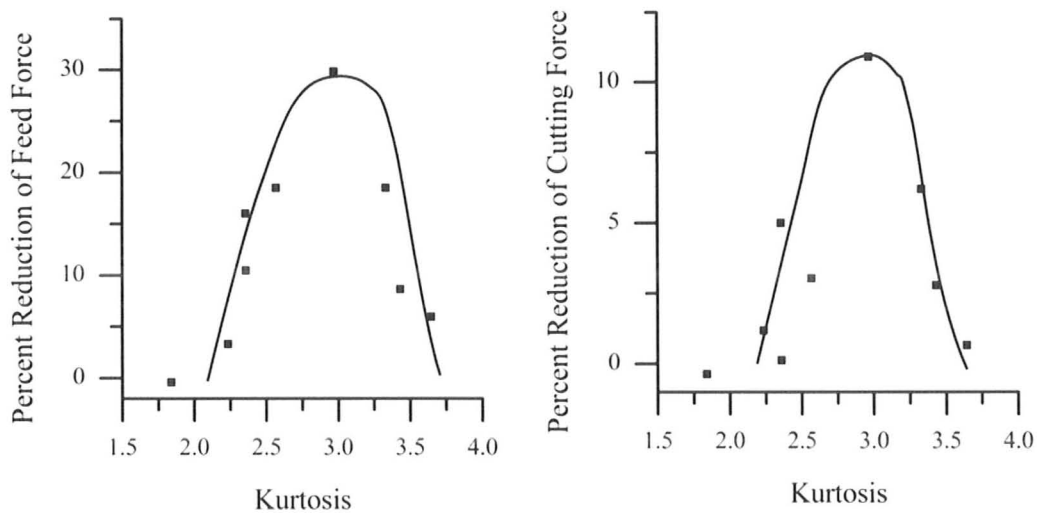


Figure 4.25. Percent Reduction of Cutting Force as a Result of EDM Surface Kurtosis - Continuous Cutting  
1045 Steel  $t = 0.1$  mm  $V_c = 2$  m/min  $X = 0.2$  mm

A trend can be seen when looking at force reduction in terms of skewness and kurtosis of the EDM surface. As seen there exists an optimum value for both skewness and kurtosis, suggesting also an optimum crater size as to be expected from all work

conducted on dimpled texturing mentioned in Chapter 2. All publications on the subject of texturing using crater shapes result in different diameter, depth, roughness, and density for each application, suggesting the process is very specific to the loads and cutting conditions experienced. As can be seen there is an optimum skewness value, being positive as in a cup shaped surface, as expected to act as a micro bearing. Any variation from the optimum value results in a decrease in effectiveness suggesting an optimum.

There is also an optimum value of kurtosis, which is a measure of the peakedness of the surface, which suggests an optimum height to width ratio. Again, this was expected as the ratio of dimple to depth is important for optimum force reduction.

## **4.6 Cutting Parameters**

The cutting parameters also have an effect on the extent of force reduction and will be discussed in the following sections:

### *4.6.1 Effect of Cutting Speed and Feed in Continuous Cutting*

To determine the range of effectiveness of a textured insert it was tested at uncut chip thickness of 0.025 and 0.05 mm and speeds of 2, 10, 25,40 and 75 m/min. It can be clearly seen in Figure 4.26 and Figure 4.27 that the inserts are effective only at low speed cutting and uncut chip thickness. Any deviation from the optimal speeds and uncut chip thickness results in a decrease in the effectiveness of the tool.

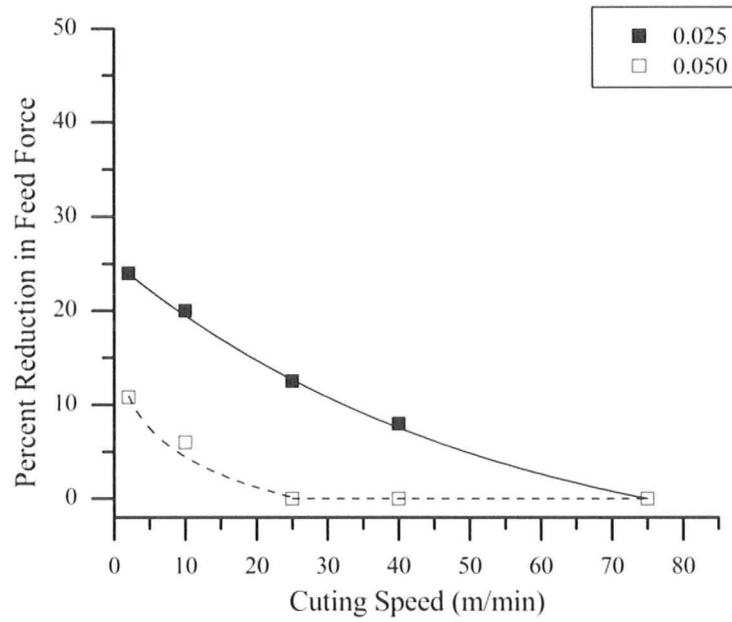


Figure 4.26. Percent Reduction in Feed Force as a Function of Uncut Chip Thickness and Cutting Speed– Continuous Cutting 1045 Steel  $X = 0.06$  mm

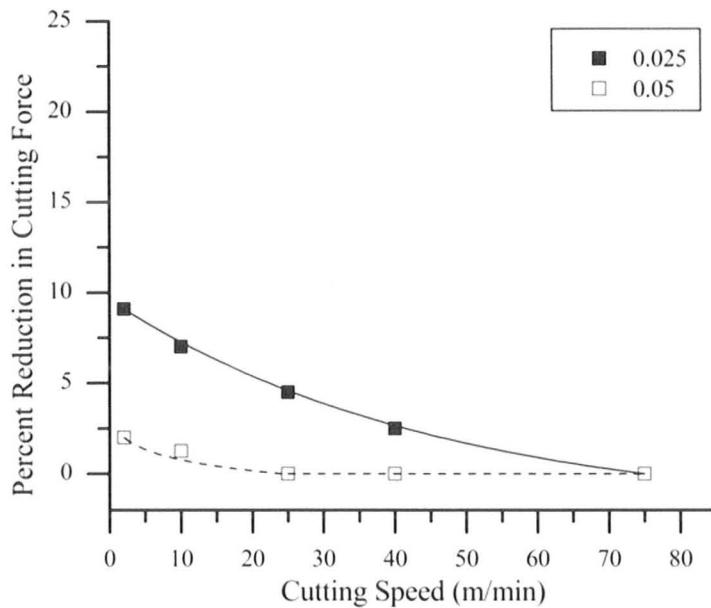


Figure 4.27. Percent Reduction in Cutting Force as a Function of Uncut Chip Thickness with an Increase in Cutting Speed– Continuous Cutting 1045 Steel  $X = 0.06$  mm

As can be seen the effectiveness of the texture decreases with increasing cutting speed as expected based on the works from Shaw, Childs [11][13][14][41], indicating the negative relation between cutting speed and lubricant effectiveness. With an increase in cutting speed the time available for penetration and reaction with the workpiece material to form a solid lubricant is now decreased. The effectiveness also decreases with increasing chip thickness as the oil penetrates less towards the cutting edge.

#### *4.6.2 Effect of Cutting Speed – Continuous and Interrupted Cutting Comparison*

A textured insert was tested at an uncut chip thickness of 0.1 mm for comparison at various cutting speeds, with initial EDM parameters and X distance of 0.2 mm, for both continuous and interrupted cutting. As can be seen in Figure 4.28, the textured surface reduces forces at all speeds tested for both continuous and interrupted cutting, and extended the range of effectiveness of the lubrication, however the effectiveness decreased with increased speed. The results also indicate the better ingress of lubricant into the tool-chip interface in the case of interrupted cutting. Due to safety concerns associated with prolonged high speed testing with lubrication, specifically the flammable nature of the lubricant, no such testing was completed past 20 m/min. It should be noted that due to the low speed nature of lubricated cutting this should not be an issue, as lubricated cutting generally operates under cutting speeds of 10 m/min [16][17][18].

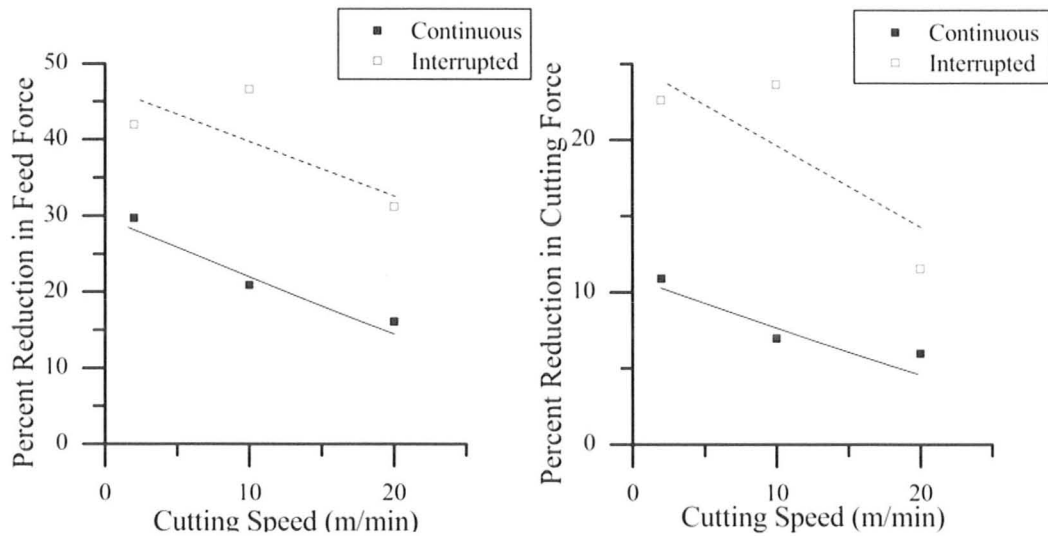


Figure 4.28 Percent Reduction in Feed and Cutting Force as a Function of Cutting Speed - Continuous and Interrupted Cutting 1045 Steel  $t = 0.1$  mm  $X = 0.2$  mm

#### 4.6.3 Engagement Length

The engagement length of a cut was tested using interrupted cutting at various diameter workpieces. For a single rotation of an interrupted workpiece, there are 4 cuts that occur. The engagement length referred to the length of a single cut. A sample was tested with a non textured edge length  $X$  of 0.4 mm and preliminary EDM parameters. As previously determined an edge length  $X$  of 0.4 mm would use an uncut chip thickness between 0.15 to 0.2 mm (Figure 4.14). The optimum uncut chip thickness was determined to be 0.175 mm. In continuous turning no reduction in cutting forces between the textured and non-textured samples was realized. Testing using the interrupted workpiece and utilizing a speed of 2 m/min and uncut chip thickness of 0.175 mm a considerable reduction of force was found. However the force reduction was found only

at a low level of tool engagement in the workpiece, using the workpiece of diameter 38 mm, as seen in Figure 4.29.

Table 4.5. Engagement Length of Test

<i>Diameter (mm)</i>	<i>Engagement (mm)</i>	<i>Disengagement (mm)</i>
58	32.7	12.8
48	24.8	12.9
38	16.9	12.9

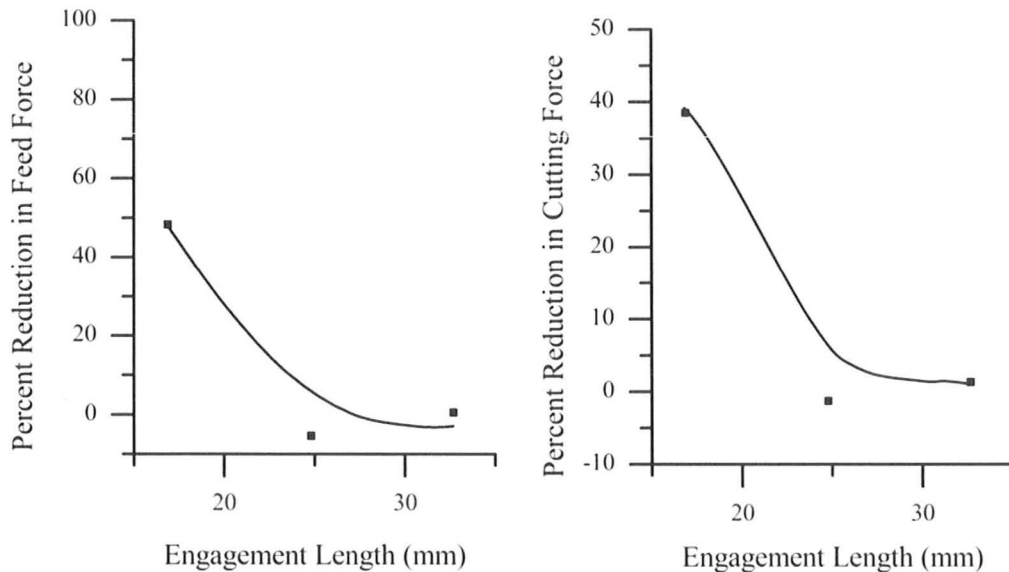


Figure 4.29. Percent Reduction in Average Feed and Cutting Force based on Length of Test – Interrupted Cutting 1045 Steel  $t = 0.1$  mm  $V_c = 2$  m/min  $X = 0.40$  mm

No reduction was noted using continuous testing. This can be explained by research conducted by Childs [9]. At an increased uncut chip thickness, lubrication penetration is minimal and loses effectiveness. However in an interrupted cut, lubricant can enter and be retained in the textured surface. During the cut the oil is transported away, as such is only effective over a finite distance before this effect is being dissipated.

#### 4.6.4 Testing on Aluminum Workpiece

A textured insert was also tested on 6061 aluminum workpiece for comparison purposes, at a cutting speed of 2 m/min and uncut chip thickness of 0.15 mm, with a non textured edge length X of 0.2 mm and initial EDM parameters. The comparison between textured and non textured inserts can be seen in Figure 4.30 and Figure 4.31. The figures show a significant reduction in both the forces and associated variability between textured and non textured inserts. It should be noted at this point that the lubricant used in this thesis was tailored towards cutting aluminum.

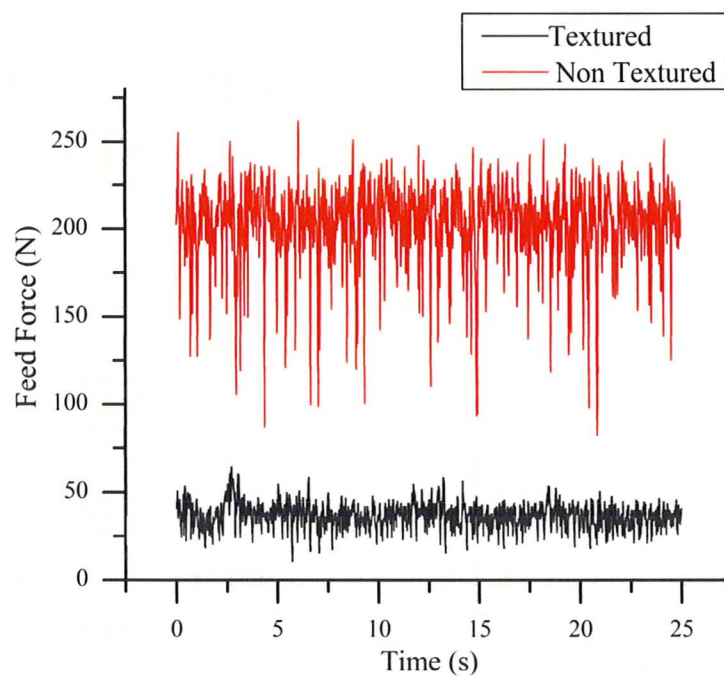


Figure 4.30. Feed Force Comparison between Textured and Non Textured Inserts – Continuous Cutting 6061 Aluminum  $t = 0.15$  mm  $V_c = 2$  m/min  $X = 0.2$  mm

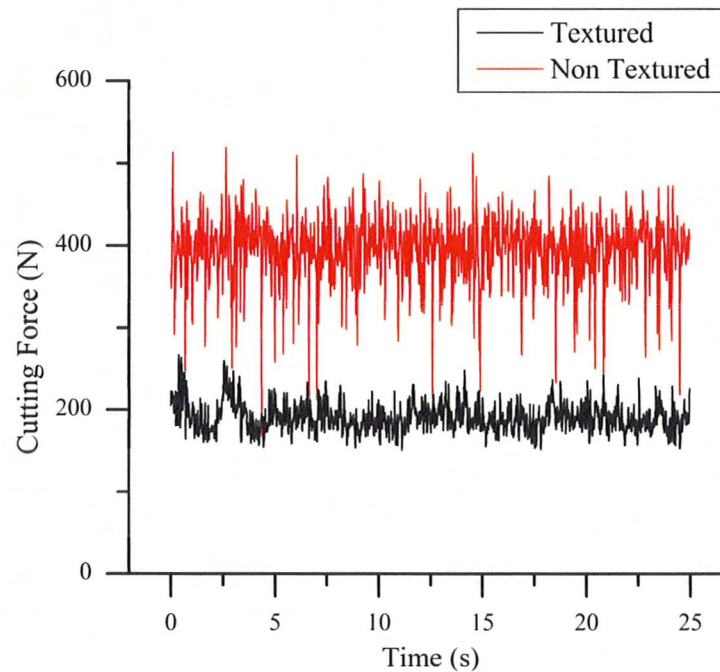


Figure 4.31 Cutting Force Comparison between Textured and Non Textured Inserts – Continuous Cutting  
6061 Aluminum  $t = 0.15$  mm  $V_c = 2$  m/min  $X = 0.2$  mm

#### 4.6.5 Texture Location When Cutting Aluminum

A test was conducted using continuous turning on a 6061 aluminum test sample at varying uncut chip thicknesses to compare with the results of using various non textured edge lengths  $X$  on steel. A textured insert with a non textured edge length  $X$  of 0.2 mm was tested at a cutting speed of 2 m/min at various uncut chip thicknesses.

Much like the variable length gap test on steel, there is an optimum uncut chip thickness as seen in Figure 4.32 that corresponds to the maximum force reduction for a given non textured gap size. For an  $X$  value of 0.2 mm, the optimum uncut chip thickness was 0.15 mm. At this uncut chip thickness the chip-tool contact length was 0.98 mm. Chip formation in aluminum is significantly different from steel as such more research is required. It is also interesting to note the reduction variation of the forces, as expected

due to the lubrication and reduction of contact length as per research by Sugihara [33] who demonstrated the anti-adherability of such textures when machining aluminum.

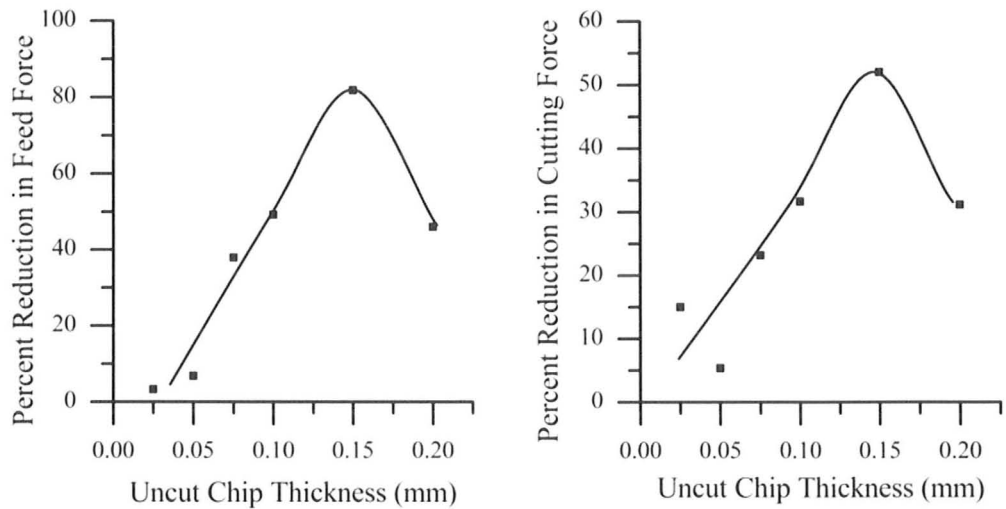


Figure 4.32 Percent Reduction in Feed and Cutting Force as a Function of Uncut Chip Thickness— Continuous Cutting 6061 Aluminum  $V_c = 2$  m/min  $X = 0.2$  mm

#### 4.7 Workpiece Surface Roughness

In addition to force reductions, the quality of the machined surface is critical in determining if the textured cutting inserts are feasible in manufacturing processes. It was found that there was no significant difference in the roughness between surfaces machined using textured and non-textured surfaces machined using textured and non textured inserts (Figure 4.33).

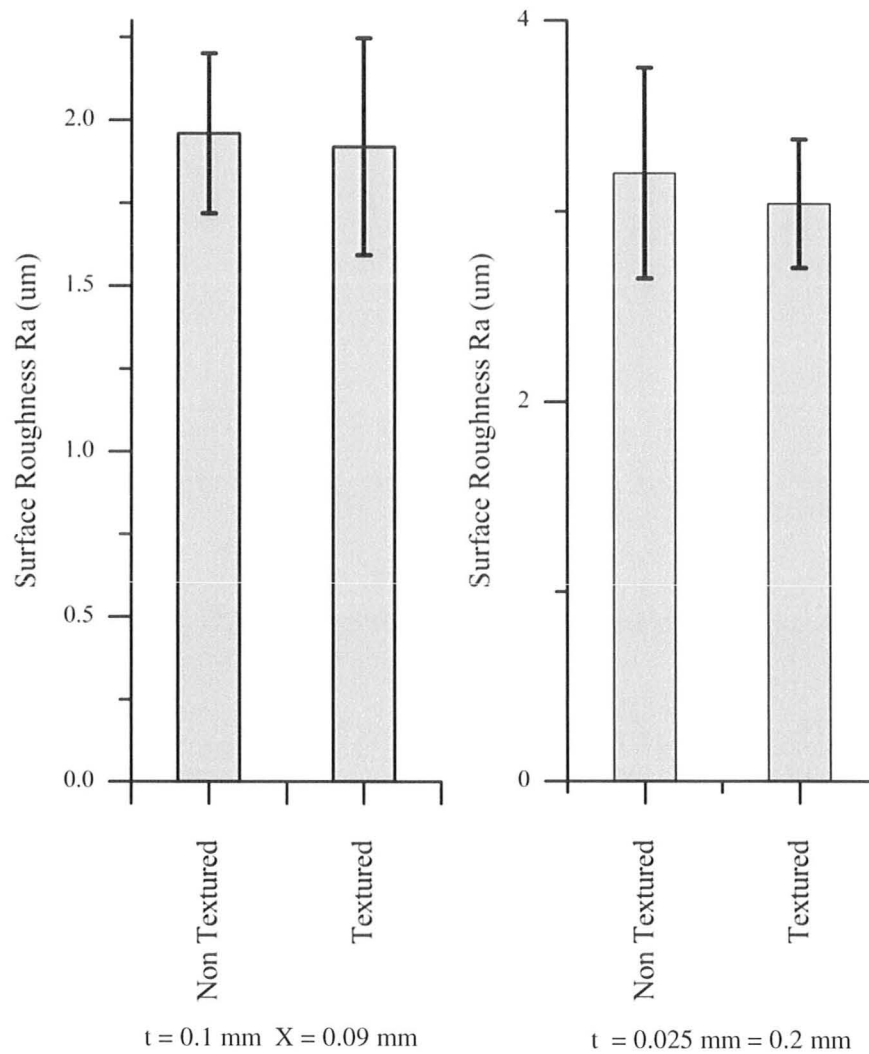


Figure 4.33 Surface Roughness Ra(um) at Different Uncut Chip Thickness– Continuous Cutting 1045 Steel  
 $V_c = 2 \text{ m/min}$

## Chapter 5

### Conclusions and Future Work

#### 5.1 Conclusion

Based on the research conducted in this thesis it can be seen that inserts textured using EDM are capable of reducing cutting forces on an average of 30% in the feed direction and 15% in the cutting direction when continuous cutting 1045 steel. Larger reductions in forces were realized in interrupted cutting: almost 50% in the feed direction and 40% in the cutting direction, at uncut chip thickness greater than that possible when using continuous cutting.

The textured tools provided some reduction in cutting forces during non lubricated cutting as well, as the tool likely acted to some degree as a restricted rake face tool.

Textured tools must be properly designed with regard to uncut chip thickness. Extension of the textured surface onto the sticking zone of the tool-chip contact length can in fact lead to an increase in cutting forces. For best results the optimum placement of the texture is close to the beginning of the sliding zone of the contact length, which is about roughly 50% of the tool-chip contact length.

The linear textured inserts showed the advantages of having the rake face of the insert completely textured as opposed to only over a finite area. Increasing reduction of forces was realized with greater area of the surface textured.

An optimum value of skewness and kurtosis corresponds to maximum reduction in forces.

Cutting parameters and workpiece material are of significance in terms of force reduction. The force reduction is maximum at low cutting speeds (on the order of 50% of feed force and 40% of cutting force) and decreases with increasing speeds. EDM textured tools are hence most beneficial in operations such as broaching. In interrupted cutting engagement length is important at higher (on the order of 0.175 mm) uncut chip thickness, as maximum force reduction occurs at smaller cutting lengths. The tools must also be designed for specific materials with respect to location of the texture, as noticed when cutting 6061 aluminum whose chip formation characteristics are different from that of 1045 steel.

Lubricant application direction was found to be largely unimportant as under essentially flood lubricant condition the capillary action was almost instantaneous in promoting the ingress of the lubricant into the tool-chip contact zone.

No change in surface roughness between surfaces machined using textured and non textured tools was noticed.

EDM creates surfaces with thermal stresses and cracks that render them prone to surface cracking. Initially the edge of the cutting insert was left intact with no texturing for this reason, however, the additional benefits of force reduction quickly became apparent. During testing one of the cutting edges fractured catastrophically most likely due to these affects. For future testing it should be included that there is the possibility of fracture of inserts textured using EDM due to the cracks and thermal stresses. For large

scale production the texture should hence is better generated during the die compacting process.

## **5.2 Future Work**

At low uncut chip thicknesses, usually 0.1 mm and smaller, the chip formation was primarily continuous; however at larger uncut chip thicknesses the possibilities of discontinuous chip formation was realized. This was due to the size and stability of the workpiece used for testing, and any deflections in the test setup. During operation smaller diameter workpieces were able to bend and deflect more than larger diameter workpieces, giving rise to more discontinuous chip formation. This should be noted for future testing, for comparable results continuous chip formation must be present in all cases, which lead to the most favorable results for the cutting tools.

Future work could investigate the use of solid lubricants that can be applied directly to the textured surface. As lubricants are expensive and environmentally sensitive, solid lubricants such as graphite may be applied specifically in interrupted cutting as they have shown to be effective. In operations such as broaching and tapping where a solid lubricant could easily be applied during cuts this may prove to be beneficial in terms of both force reduction, and reducing costs associated with liquid lubricants. As determined, the tooling, texturing and process must be optimized for all cutting conditions including the specific lubricant.

High speed cutting may also be considered. In most high speed cutting operations coolants are used as opposed to lubricants, which would not be beneficial in providing

force reduction on materials such as steel, however it may be beneficial for materials such as aluminum which experience high adhesion. In an operation such as milling where the cuts are interrupted the ability of coolants to penetrate and be retained in the texture increases, thus possibly impeding the tendency of the work material to adhere to the tool surface.

A correlation between dimple parameters, material parameters, and operating conditions may be determined with extensive research and should be considered to provide a database of conditions where texturing may be beneficial.

A wear test was considered to compare tool life between textured and non textured tools. Unfortunately the test cannot be accelerated due to the very specific uncut chip thickness and cutting speeds required for the texture to reduce forces. As such the test requires a considerable amount of time and material. A reduction in forces though should lead to a reduction in wear and thus an improvement in tool life. If a textured tool is to be considered for industrial applications some thought must be given to tool life, perhaps coupled with a coating to further improve tool life. Wear of the texture over time should also be considered to determine how the shape of the texture changes and if the lubrication properties of the textures changes with use.

## References

- [1] Gosh, A. Mallik, A. (1985). *Manufacturing Science*. New Delhi Affiliated East – West Press Ltd.
- [2] Nachtman, Elliot. (1985). *Lubricants and Lubrication in Metalworking Operations*. New York: Marcel Dekker Inc.
- [3] Holmber, K., Matthews, A. (1994) *Coatings Tribology: Properties, Techniques and Applications in Surface Engineering* Netherlands : Elsevier Science B.V.
- [4] Classical Friction. *Electronic Reference*. Retrieved 08-11-2008, from <http://calcul.com/ian/thesis/node21.html>
- [5] Williams, John. (2005). *Engineering Tribology*. New York: Cambridge University Press.
- [6] A. Mallock, The Action of Cutting Tools, Proceedings of the Royal Society of London 33(1881-1882) 127-139.
- [7] T. Wakanayashi et al, The Kinetics of gas – phase lubrication in the orthogonal machining of an aluminum alloy. *Journal of Engineering Tribology* 209(2)(1995) 131-136.
- [8] E. Doyle, J. Horne, Frictional Interaction between Chip and Rake Face in Continuous Chip Formation, Proceedings of the Royal Society of London, Series A, Mathematical and Physical Sciences 1979 (366) 173-183.
- [9] T. Childs, Friction Modeling in Metal Cutting. *Wear* 260 (2006) 310-318.
- [10] M.B. da Silva et al. Lubrication and Application Method in Machining. *Industrial Lubrication and Tribology*, 50 (4)(1998) 149-152.
- [11] Childs. T.H.C, (2000) *Metal Machining: Theory and Applications*, Boston: Butterworth-Heinemann.
- [12] T. Smith et al, Theoretical Analysis of Cutting Fluid Interaction in Machining, *Tribology International* 21(5)(1988) 239-244.

- [13] J.A. Williams, The Action of Lubricants in Metal Cutting, *Journal of Mechanical Engineering Science* 19 (1977) 202-212.
- [14] L. De Chiffre, Mechanics of Metal Cutting and Cutting fluid Action. *International Journal of Machine Tool Design and Research* 17(1977) 225-234.
- [15] T. Shirakashi et al, The Conflicting Roles of Carbon tetrachloride as a Boundary Lubricant, *Journal of Engineering for Industry* 100 (1978) 244-248.
- [16] R.B. Schroeter et al, Simulation of the Main Cutting Force in Crankshaft Turn Broaching, *International Journal of Machine Tools and Manufacture* 47 (2007) 1884 -1892.
- [17] J.W. Sutherland et al, A model for the Cutting Force System in the Gear Broaching Process. *International Journal of Machine Tools and Manufacture* 37(10)(1997) 1409-1421.
- [18] T. Cao, J. Sutherland, Investigation of Thread Tapping Load Characteristics Through Mechanistic Modeling and Experimentation, *International Journal of Machine Tools and Manufacture* 42(2002) 1527-1538.
- [19] A. Erdemir. Review of engineered tribological interfaces for improved boundary lubrication. *Tribology International* 38(2005) 249-256.
- [20] A. Kovalchenko et al. The Effect of Laser Texturing of Steel Surfaces and Speed Load Parameters on the Transition of Lubrication Regime from Boundary to Hydrodynamic. *Tribology Transactions* 47(2004) 299-307
- [21] Laser Surface Texturing. *Electronic Reference*. Retrieved 8-11-2008, from <http://www.advancedsealingsolutions.com/images/lst.jpg>
- [22] G. Ryk et al. Experimental Investigation of Laser Surface Texturing for Reciprocating Automotive Components. *Tribology Transactions* 45(2002) 444-449.
- [23] L.M. Vilhena et al, Surface Texturing by Pulsed Nd: YAG Laser, *Tribology International* 42(2009) 1496-1504

- [24] I. Etsion, State of the Art in Laser Surface Texturing. *Journal of Tribology*. 127 (2005) 248-254.
- [25] D. Zhu et al. Electrochemical micromachining of microstructures of micro hole and dimple array. *CIRP Annals – Manufacturing Technology* 58(2009) 177-180.
- [26] S. Qian, Generating micro-dimples array on the hard chrome-coated surface by modified through mask electrochemical micromachining, *International Journal of Advanced Manufacturing Technology* 47 (2010) 1121-1127 .
- [27] L. Galda et al, Dimples shape and distribution effect on characteristics of stribeck curve. *Tribology International* 42(2009) 1505-1512.
- [28] A. Voevodin, J. Zabinski, Laser Surface Texturing for Adaptive Solid Lubrication. *Wear* 261(2006) 1285-1292.
- [29] W. Jiang et al, Bio-mimetic surface structuring of coating for tribological applications. *Surface Coatings Technology* 201(2007) 7889-7895.
- [30] U. Pettersson, S. Jacobson, Textured Surfaces for improved lubrication at high pressure and low sliding speed of roller/piston in hydraulic motors. *Tribology International* 40(2)(2007) 355-359.
- [31] H.L. Costa, I.M. Hutchings, Effects of Die Surface Patterning on Lubrication in Strip Drawing, *Journal of Materials Processing Technology* 209 (3)(2009) 1175-1180.
- [32] N. Kawasegi, H. Sugirmori, Development of Cutting Tools with Microscale, NanoScale Textures to Improve Frictional Behavior. *Precision Engineering* 33(2009) 248-254.
- [33] T. Sugihara, T. Enomoto, Development of a Cutting Tool with a Nano/Micro Textured surface- Improvement of anti-adhesive effect by considering the texture patterns, *Precision Engineering* 33(2009) 425-429.
- [34] P. Berlet et al. The Effect of Sample Finishing on the Tribology of metal/metal lubricated contacts. *Wear* 268 (2010) 1518-1523.
- [35] V. Franzen et al, Textured Surfaces for Deep Drawing Tools by Rolling. *International Journal of Machine Tools and Manufacture* (2010) In Press.

- [36] D. Jianxin et al. Design, fabrication and properties of a self-lubricated tool in dry cutting. *International Journal of Machine Tools and Manufacture* 49(2009) 66-72.
- [37] D. Scott et al. Analysis and Optimization of Parameter Combinations in Wire Electrical Discharge Machining. *International Journal of Production Research* 29(11)(1991) 2189-2207.
- [38] T. Spedding, Z. Wang, Study of Modeling of Wire EDM Process. *Journal of Materials Processing Technology* 69 (1997) 18-28 .
- [39] S. Kumar et al, Surface Modification by Electrical Discharge Machining: A review. *Journal of Materials Processing Technology* 209(2009) 3675-3687.
- [40] I. Menzies. *Abrasion Assisted Wire Electrical Discharge Machining*, 2007, M.A.Sc Thesis, McMaster University.
- [41] M.C. Shaw, On the Action of Metal Cutting Fluids at Low Speeds. *Wear* (2) 1959 217-227.
- [42] A. Bruzzone, et al, Advances in Engineered Surfaces for Functional Performances. *CIRP Annals – Manufacturing Technology* 57(2008) 750-769
- [43] El-Hofy, H.(2005) *Advanced Machining Processes*. New York : McGraw-Hill Professional
- [44] High Performance EDM Machining. *Electronic Reference*. Retrieved 8-11-2008 from <http://www.wirecut-co.com/capabilities.asp>
- [45] Stephenson, D. (1997) *Metal Cutting Theory and Practice*. New York: Marcel Dekker
- [46] Shaw, M. (1984) *Metal Cutting Principles*. New York: Oxford Press.
- [47] Boisse, P., Altan, T. (2003) Luttervelt, K. *Friction and Flow Stress in Forming and Cutting*. Sterling VA : Kogan Page Science.
- [48] S. Pandit, K. Rajurkar, Crater Geometry and Volume From Electro Discharge Machined Surface Profiles by Data Dependent Systems. *Journal of Engineering for Industry* 102 (1980) 189-195.

- [49] Boothroyd, G. Knight, W. (1989) *Fundamentals of Machining and Machine Tools*. New York: Marcel Dekker Inc.
- [50] Trent, E., Wright, P.,(2000) *Metal Cutting*. Boston: Butterworth Heinenmann.
- [51] P. Pawlus et al, Abrasive wear resistance of textured steel rings. *Wear* 267 (2009) 1873-1882.
- [52] M. Stanford et al. The future role of metalworking fluids in metal cutting operations, *Industrial Lubrication and Tribology*, 54 (2002) 11-19.
- [53] Z.M. Hu, T.A. Dean. A Study of Surface Topography, friction and lubricants in metalforming, *International Journal of Machine Tools and Manufacture* 40 (2000) 1637-1649.
- [54] J. Bailey, Friction in Metal Machining - Mechanical Aspects. *Wear* (31) (1975) 243-275.
- [55] T. Childs, et al. Physics in metal Cutting, *Report on Progress in Physics*, 36 (1973) 223-288.
- [56] P.J. Blau et al, Effects of Surface Grinding Conditions on the Reciprocating Friction Wear Behavior of Silicone Nitride, *Wear* 203-204 (1997) 648-657.
- [57] P.M. Lonardo et al, Effect of Flushing and Electrode Material on Die Sinking EDM, *CIRP Annals* 48 (1999) 123-126